This effect in the TrkB-transformant cells was dependent on the dose of BDNF (Fig. 3J). Western blot analysis showed that two signal-transduction factors in a TrkB down-stream, extracellular signal-regulated kinase (ERK) and MAPK/ERK kinase (MEK), were phosphorylated by BDNF treatment in the TrkB transformant, but not in the mock transformant cells (Fig. 3K), which demonstrates that the TrkB transformant has a normally functioning TrkB protein, while the mock transformant does not. These results indicate that TrkB is necessary for the acceleration of methylmercury-induced cell death or for the increase of cell viability through BDNF treatment.

3. Discussion

This is the first study documenting that BDNF aggravates the neuronal death induced by an environmental toxin, methylmercury, although BDNF is included in the NGF family. We demonstrated that BDNF and NT-4 accelerate the methylmercury-induced cell death of rat cerebellar granule cells in primary cultures in a dose-dependent manner, but that NGFβ does not, which is supported by the evidence that primary cultured cells expressed a high level of TrkB but not TrkA mRNA, because the neurotrophins need to bind to specific receptors in order to achieve their cell death-accelerating effects (Bibel and Barde, 2000; Reichardt, 2006). The experiment using a neutralizing antibody against BDNF also proved the necessity of BDNF binding to TrkB for the effect of BDNF as an accelerator of methylmercury-induced cell death. Furthermore, the methylmercury-induced death in the TrkB transformant of rat neuroblastoma cell line B35 was accelerated by BDNF treatment, but not that in the mock transformant. These results indicate that TrkB activation by BDNF is responsible for the accelerating effect on methylmercury-induced cell death. Among Trks, the cells of the primary culture expressed only TrkB in the present study. Therefore, as TrkB is a receptor of BDNF, only BDNF should have been an accelerating factor against methylmercury-induced cell death among neurotrophins. Had TrkA or TrkC been expressed in the primary culture, NGF or NT-3 might have induced an acceleration of methylmercury-induced cell death, because TrkA and TrkC can process signal transduction through at least three signaling pathways, MAPK, PLC γ, and PI3K, that TrkB also processes (Bibel and Barde, 2000; Reichardt, 2006). However, the results of the present study did not sufficiently clarify whether TrkA and TrkC are involved in the accelerating effect on methylmercury-induced cell death in the manner of TrkB. To resolve these questions, more experiments will be needed to observe the effects of NGFβ on methylmercury-induced death in TrkA-expressing cells, such as rat adrenal pheochromocytoma PC-12 cells.

When the cytotoxicity of methylmercury did not appear, BDNF functioned as a neurotrophin for both the primary cultured neurons of the cerebellum and the TrkB transformant of B35 cells co-treated with methylmercury and BDNF. However, when the cell viability was decreased by methylmercury toxicity, BDNF functioned as an accelerator of the methylmercury-induce cell death (Figs. 1 and 3). These results indicate that BDNF exhibits not only trophic activity, but also death acceleration activity, and thus that the role of BDNF is altered by the appearance of methylmercury cytotoxicity.

There may be cross-talk mechanisms between the BDNF and methylmercury pathways. In primary cultured neurons from mice cerebella, methylmercury shows its neurotoxicity by increases in intracellular Ca^{2+} concentrations through NMDA receptor activation, and the toxicity is suppressed with NMDA receptor antagonists (Park et al., 1996). The disappearance of methylmercury neurotoxicity by treatment with NMDA receptor antagonists has also been observed in an in vivo study (Miyamoto et al., 2001). Using the same culture system used in the present study, we previously showed that methylmercury induces an increase in intracellular Ca^{2+} concentrations, which in turn activates calpain, a Ca^{2+} concentration-dependent protease, to play its role in methylmercury-induced cell death (Sakaue et al., 2005). BDNF phosphorylates NMDA receptors via TrkB, resulting in a slight increase in intracellular Ca^{2+} concentrations, but the levels of intracellular Ca^{2+} concentrations should still be low compared to the levels of intracellular Ca^{2+} concentrations increased by methylmercury. This BDNF effect on the intracellular Ca^{2+} concentrations is suppressed by treatment with a kinase inhibitor against Trks, K-252a, or an NMDA receptor antagonist, MK-801 (Xu et al., 2006; Sanchez-Perez et al., 2006). As shown above, U0126 also inhibited the effects of methylmercury and BDNF (Fig. 2B). Moreover, we determined that a subtype of the NMDA receptor, NR1, is phosphorylated by BDNF or NT-4 treatment, but not by NT-3 in our primary culture system (data not shown). Thus, BDNF might realize its acceleration of methylmercury-induced cell death by stimulating a methylmercury-induced increase of intracellular Ca^{2+} concentration. However, confirmation of this proposed mechanism is beyond the scope of the present study. Further studies using Ca^{2+} indicators or endogenous markers for increases in Ca^{2+} concentrations will be needed in order to detect any augmentation of intracellular Ca^{2+} concentrations by BDNF treatment.

In conclusion, the present results indicate that BDNF exacerbates methylmercury-induced cell death via TrkB, indicating that BDNF and TrkB are factors regulating the sensitivity to methylmercury cytotoxicity. The neurotoxicity of methylmercury has at least two toxicological characteristics, as follows. First, fetuses and infants show a higher sensitivity to methylmercury than adults (Takeuchi, 1968; Bakir et al., 1973; Harada, 1968; Marsh et al., 1980). BDNF is indispensable for the development of normal structures, as well as for cell survival and function, in the nerve tissue of developing animals such as fetuses and infants (Sinder, 1994; Bibel and Barde, 2000). If the effect of BDNF as an accelerator, not as a neurotrophin, on the methylmercury-induced cell death in vitro is also detected in the brain, the indispensability of BDNF for normal development of nerve tissue might determine the higher sensitivity to methylmercury in developing animals. The second characteristic is that neurons highly sensitive to methylmercury toxicity, such as cerebellar granular cells and granular cells of the cerebral cortex, are in particular areas of the central nervous system (Tsubaki and Irukayama, 1977; Weiss et al., 2002), which means that the difference in sensitivity to methylmercury occurs between neurons even in the same brain. In the present study, BDNF

promoted methylmercury-induced death of TrkB-expressing cells, suggesting that neurons which express TrkB will be more sensitive to methylmercury than those which do not. Thus, the difference in methylmercury sensitivity between neurons in the brain may be determined by whether or not individual neurons express TrkB. And in fact, the second to fifth layers of the cerebral cortex of humans show higher levels of TrkB mRNA, while the second and following layers show a higher expression of BDNF mRNA (Webster et al., 2006), which is in partial agreement with the layers of the human cerebral cortex that are degenerated by methylmercury exposure, particularly the second and third layers (Takeuchi et al., 1977). The BDNF-induced acceleration of methylmercury-induced cell death is a good model to clarify the mechanisms of this BDNF effect. Further investigation using this model may help to identify the mechanisms and characteristics of methylmercury toxicity.

4. Experimental procedures

4.1. *Cell cultures and treatment*

Primary cultures of cerebellar granule neurons were prepared from Wistar rats (Jcl:Wistar; Clea Co., Tokyo, Japan) within 24 h after birth, as described previously (Sakaue et al., 2005). Briefly, cerebella were removed from the pups and incubated with trypsin for 13 min at room temperature were minced by mild triturating with a Pasteur pipette. Cerebellar granule cells were seeded in Eagle's minimal essential medium (Gibco BRL, Grand Island, NY) containing 1 mg/ml BSA, 10 μg/ml bovine insulin, 0.1 nM thyroxin, 0.1 μg/mg human transferrin, 1 μg/ml aprotinin, 30 nM Na_2SeO_3, 0.25% glucose, 100 U/mL penicillin, and 135 μg/mL streptomycin on poly-L-lysine-coated dishes and cultured for 2 days. Rat neuroblastoma B35 cells were purchased from the American Type Culture Collection (ATCC, Manassas, VA). The B35 cells were cultured in growth medium, Dulbecco's modified Eagle's medium supplemented with 10% fetal calf serum (HyClone, South Logan, UT), 100 U/mL penicillin, and 135 μg/mL streptomycin. The medium was changed every second day. These cell culture supplements were purchased from Sigma-Aldrich (St. Louis, MO).

The cells were pre-incubated for 24 h and treated with methylmercuric chloride (Tokyo Kasei Kogyo. Co., Ltd., Tokyo, Japan) at the concentrations indicated in the figures with or without recombinant human BDNF (Peprotech, London, UK), recombinant human neurotorophin-4 (NT-4; Sigma-Aldrich), or mouse nerve growth factor (NGFβ; Sigma-Aldrich). These neurotrophins were added to the medium 30 min before the methylmercury treatment. In addition, a BDNF-neutralizing antibody (Sigma-Aldrich) and a MAPK inhibitor, U0126 (Calbiochem, Darmstadt, Germany), were used to investigate whether the BDNF effect involves the binding of BDNF to its receptor and activation of the MAP signaling cascade. The numbers of viable cells of the primary culture and the B35 cell line were estimated by crystal violet staining, as described previously (Sakaue et al., 2005). All experiments were carried out in accordance with the Kitasato University Guidelines for Animal Care and Experimentation.

4.2. *Cloning of the stable transformant of B35 cells expressing TrkB*

Using two primers, rTrkB1FEcoRI (5′-GAATTCCTGGCGTATAGG-AC-3′) and rTrkB1RNotI (5′-GCGGCCGCACTGTCAGAGCGAA-3′), designated on the sequences of rat TrkB from GenBank (Accession No. NM_012731), rat TrkB cDNA was amplified with rat brain cDNA as a template. An approximately 2.8-kb cDNA fragment of TrkB was cloned into the EcoRI/NotI site of pcDNA3.1 (Invitrogen, Carlsbad, CA) for construction of the expression plasmid and then sequenced.

B35 cells were transfected with the TrkB expression construct using Lipofectamin (Invitrogen, Carlsbad, CA) according to the manufacturer's instructions. Stable transformants were selected in growth medium containing 0.8 mg/ml geneticin (G418; Invitrogen). G418-resistant cells were cloned, and the TrkB mRNA expression was checked in each clone using RT-PCR. To confirm the function of the expressed TrkB protein in the transformant, phosphorylation of two factors of signal transduction in the region down-stream of TrkB, ERK and MEK, in the selected clone in mock or TrkB transformants after BDNF treatment was detected using Western blot analysis, which was performed as described in our previous report (Sakaue et al., 2005). Briefly, after BDNF treatment at 50 ng/ml, B35 cells were washed three times with PBS (pH 7.4) and harvested in Lamini's buffer (3% SDS, 62.5 mM Tris base, pH 6.8). The protein concentration in cell lysates was determined by a BCA assay (Bio-Rad, Hercules, CA). SDS-polyacrylamide gel electrophoresis (PAGE) was performed with 50 μg of lysate protein. For Western blotting, proteins were transferred to a PVDF membrane (GE Healthcare, Buckinghamshire, UK) at 100 V for 2 h. To determine the phosphorylation state, the membrane was washed in 0.05% Tween-20 PBS (T-PBS) and incubated in a blocking buffer, 1% bovine serum albumin T-PBS, for 1 h at room temperature. Then, the first antibody, i.e., rabbit anti-phospho-ERK (pERK) 1/2 antibody, anti-ERK1/2 antibody, anti-phospho-MEK antibody or anti-MEK antibody, was reacted with the membrane for 12 h at 4 °C, followed by reaction with horseradish peroxidase-conjugated secondary antibody (1:1000; Sigma) for 1 h at 4 °C. These antibodies were purchased from Cell Signaling Technology, Inc. (Danvers, MA). Enhanced chemiluminescence by Chemilumi one (Nacali Tesque, Kyoto, Japan) was determined by exposure to an X-ray film (GE Healthcare).

4.3. *RT-PCR*

Total RNAs of rat cerebellar neuronal culture and whole cerebella were extracted and reverse-transcribed in a reaction solution containing SuperScript™ II reverse transcriptase and $Oligo(dT)_{12\text{-}18}$Primer (Invitrogen) for producing cDNA, as described previously (Sakaue et al., 2002). The cDNAs were stocked at −20 °C before use. PCRs for TrkA, TrkB, and TrkC were carried out in 50 μl of PCR mixture containing 1.25 U of ExTaq™ polymerase (Takara Biochemicals, Otsu, Japan), 1×ExTaq™ buffer, 0.2 mM dNTP mixture, 100 pM of each primer, and 2 μl of the cDNA. The PCR conditions for all genes were as follows: an initial denaturation step at 95 °C for 3 min, followed by 40 cycles of denaturation at 95 °C for 30 s, annealing at 60 °C for 30 s, and extension at 72 °C for 45 s, with

a final extension step at 72 °C for 3 min. The primer sequences of the neurotrophin receptors reported by Nemoto et al. (2000) were referenced in the present study.

Acknowledgments

This study was supported by a grant (no. 20780221, to MS) from the Ministry of Education, Culture, Sports, Science, and Technology of Japan, by a project grant (Young Scientist Research Training Award, 2008) from the Azabu University Research Services Division (to MS), and by a grant from The Morinaga Foundation for Health and Nutrition (to MS).

REFERENCES

Aschner, M., Du, Y.L., Kimelberg, H.K., 1993. Methylmercury-induced alterations in excitatory amino acid transport in rat primary astrocyte cultures. Brain Res. 602, 181–186.

Bakir, F., Damluji, S.F., Amin-Zaki, L., Murtadha, M., Khalidi, A., al-Rawi, N.Y., Tikriti, S., Dahahir, H.I., Clarkson, T.W., Smith, J.C., Doherty, R.A., 1973. Methylmercury poisoning in Iraq. Science 191, 230–241.

Bibel, M., Barde, Y.A., 2000. Neurotrophins: key regulators of cell fate and cell shape in the vertebrate nervous system. Genes Dev. 14, 2919–2937.

Castoldi, A.F., Barni, S., Turin, I., Gandini, C., Manzo, L., 2000. Early acute necrosis, delayed apoptosis and cytoskeletal breakdown in cultured cerebellar granule neurons exposed to methylmercury. J. Neurosci. Res. 60, 775–787.

Dare, E., Gotz, M.E., Zhivotovsky, B., Manzo, L., Ceccatelli, S., 2000. Antioxidants J811 and 17beta-estradiol protect cerebellar granule cells from methylmercury-induced apoptotic cell death. J. Neurosci. Res. 62, 557–565.

Harada, Y., 1968. Congenital (or fetal) Minamata disease. Minamata Disease. Kumamoto University, Kumamoto, pp. 93–118.

Marsh, D.O., Myers, G.J., Clarkson, T.W., Amin-Zaki, L., Tikriti, L., Majeed, M.A., 1980. Fetal methylmercury poisoning: clinical and toxicological data on 29 cases. Ann. Neurol. 7, 348–353.

Marty, M.S., Atchison, W.D., 1997. Pathways mediating Ca^{2+} entry in rat cerebellar granule cells following in vitro exposure to methylmercury. Toxicol. Appl. Pharmacol. 147, 319–330.

Miyamoto, K., Nakanishi, H., Moriguchi, S., Fukuyama, N., Eto, K., Wakamiya, J., Murao, K., Arimura, K., Osame, M., 2001. Involvement of enhanced sensitivity of N-methyl-D-aspartate receptors in vulnerability of developing cortical neurons to methylmercury neurotoxicity. Brain. Res. 901, 252–258.

Nemoto, K., Miyata, S., Nemoto, F., Yasumoto, T., Murai, U., Kageyama, H., Degawa, M., 2000. Gene expression of neurotrophins and their receptors in lead nitrate-induced rat liver hyperplasia. Biochem. Biophys. Res. Commun. 275, 472–476.

Park, S.T., Lim, K.T., Chung, Y.T., Kim, S.U., 1996. Methylmercury-induced neurotoxicity in cerebral neuron culture is blocked by antioxidants and NMDA receptor antagonists. Neurotoxicol. 17, 37–46.

Reichardt, L.F., 2006. Neurotrophin-regulated signaling pathways. Phil. Trans. R. Soc. B 361, 1545–1564.

Sakaue, M., Ishimura, R., Kurosawa, S., Fukuzawa, N.H., Kurohmaru, M., Hayashi, Y., Tohyama, C., Ohsako, S., 2002. Administration of estradiol-3-benzoate down-regulates the expression of testicular steroidogenic enzyme genes for testosterone production in the adult rat. J. Vet. Med. Sci. 64, 107–113.

Sakaue, M., Okazaki, M., Hara, S., 2005. Very low levels of methylmercury induce cell death of cultured rat cerebellar neurons via calpain activation. Toxicology 213, 97–106.

Sakaue, M., Adachi, T., Okazaki, M., Nakamura, H., Mori, N., Hara, S., Sakabe, K., 2006. Effects of sodium selenite on methylmercury-induced cell death and on mercury accumulation in rat cerebellar neurons in primary culture. Bull. Environ. Contam. Toxicol. 77, 779–784.

Sakaue, M., Mori, N., Okazaki, M., Ishii, M., Inagaki, Y., Iino, Y., Miyahara, K., Yamamoto, M., Kumagai, T., Hara, S., Yamamoto, M., Arishima, K., 2008. Involvement of independent mechanism upon poly(ADP-ribose) polymerase (PARP) activation in methylmercury cytotoxicity in rat cerebellar granule cell culture. J. Neurosci. Res. 86, 3427–3434.

Sanchez-Perez, A.M., Llansola, M., Felipo, V., 2006. Modulation of NMDA receptors by AKT kinase. Neurochem. Inter. 49, 351–358.

Sarafian, T., Verity, M.A., 1991. Oxidative mechanisms underlying methylmercury neurotoxicity. Int. J. Dev. Neurosci. 9, 147–153.

Sinder, W.D., 1994. Functions of the neurotrophins during nervous system development: what the knockouts are teaching us. Cell 77, 627–638.

Takeuchi, T., 1968. Pathology of Minamata disease. Minamata Disease. Kumamoto University, Kumamoto, pp. 141–228.

Webster, M.J., Herman, M.M., Kleinman, J.E., Weickert, C.S., 2006. BDNF and trkB mRNA expression in the hippocampus and temporal cortex during the human lifespan. Gene Expression Patterns 6, 941–951.

Weiss, B., Clarkson, T.W., Simon, W., 2002. Silent latency periods in methylmercury poisoning and in neurodegenerative disease. Env. Health Perspect. 110 (suppl 5), 851–854.

Xu, F., Plummer, M.R., Len, G.W., Nakazawa, T., Yamamoto, T., Black, I.B., Wu, K., 2006. Brain-derived neurotrophic factor rapidly increases NMDA receptor channel activity through Fyn-mediated phosphorylation. Brain Res. 1121, 22–34.

Bj www.biochemj.org

Biochem. J. (2010) 425, 361–371 (Printed in Great Britain) doi:10.1042/BJ20090045

online data

Microsomal prostaglandin E synthase-1 in both cancer cells and hosts contributes to tumour growth, invasion and metastasis

Daisuke KAMEI*†, Makoto MURAKAMI*‡§, Yuka SASAKI*, Yoshihito NAKATANI*, Masataka MAJIMA‖, Yukio ISHIKAWA¶, Toshiharu ISHII¶, Satoshi UEMATSU**, Shizuo AKIRA**, Shuntaro HARA*[1] and Ichiro KUDO*[2]

*The Department of Health Chemistry, School of Pharmacy, Showa University, 1-5-8 Hatanodai, Shinagawa-ku, Tokyo 142-8555, Japan, †Department of Research and Development for Innovative Medical Needs, School of Pharmacy, Showa University, 1-5-8 Hatanodai, Shinagawa-ku, Tokyo 142-8555, Japan, ‡Tokyo Metropolitan Institute of Medical Science, 2-1-6 Kamikitazawa, Setagaya-ku, Tokyo 156-8506, Japan, §PRESTO, Japan Science and Technology Agency, 4-1-8 Honcho Kawaguchi, Saitama 332-0012, Japan, ‖Department of Pharmacology, School of Medicine, Kitasato University, 1-15-1 Kitasato, Sagamihara, Kanagawa 228-8555, Japan, ¶Department of Pathology, School of Medicine, Toho University, 5-21-16 Omori-Nishi, Ohta-ku, Tokyo 143-8540, Japan, and **Department of Host Defense, Research Institute for Microbial Diseases, Osaka University, 3-1 Yamada-oka, Suita, Osaka 565-0871, Japan

mPGES-1 (microsomal prostaglandin E synthase-1) is a stimulus-inducible enzyme that functions downstream of COX (cyclo-oxygenase)-2 in the PGE_2 (prostaglandin E_2)-biosynthesis pathway. Although COX-2-derived PGE_2 is known to play a role in the development of various tumours, the involvement of mPGES-1 in carcinogenesis has not yet been fully understood. In the present study, we used LLC (Lewis lung carcinoma) cells with mPGES-1 knockdown or overexpression, as well as mPGES-1-deficient mice to examine the roles of cancer cell- and host-associated mPGES-1 in the processes of tumorigenesis *in vitro* and *in vivo*. We found that siRNA (small interfering RNA) silencing of mPGES-1 in LLC cells decreased PGE_2 synthesis markedly, accompanied by reduced cell proliferation, attenuated Matrigel™ invasiveness and increased extracellular matrix adhesion. Conversely, mPGES-1-overexpressing LLC cells showed increased proliferating and invasive capacities. When implanted subcutaneously into wild-type mice, mPGES-1-silenced cells formed smaller xenograft tumours than did control cells. Furthermore, LLC tumours grafted subcutaneously into mPGES-1-knockout mice grew more slowly than did those grafted into littermate wild-type mice, with concomitant decreases in the density of microvascular networks, the expression of pro-angiogenic vascular endothelial growth factor, and the activity of matrix metalloproteinase-2. Lung metastasis of intravenously injected LLC cells was also significantly less obvious in mPGES-1-null mice than in wild-type mice. Thus our present approaches provide unequivocal evidence for critical roles of the mPGES-1-dependent PGE_2 biosynthetic pathway in both cancer cells and host microenvironments in tumour growth and metastasis.

Key words: knockout mouse, metastasis, microsomal prostaglandin E synthase-1, prostaglandin E_2, tumorigenesis.

INTRODUCTION

Numerous studies on rodent cancer models and human cancers have shown that NSAIDs (non-steroidal anti-inflammatory drugs) have antineoplastic properties [1]. A well-known effect of the NSAIDs is their ability to inhibit the enzyme COX (cyclo-oxygenase) and thereby to suppress PG (prostaglandin) synthesis. PGE_2, the most common PG, is involved in tumour progression by inducing angiogenesis, invasion and metastasis in several solid tumours [2]. Biosynthesis of PGE_2 from arachidonic acid, which is spatiotemporally supplied from membrane phospholipids by the action of phospholipase A_2, is catalysed sequentially by COX and PGES (PGE synthase) [3]. COX catalyses the insertion of molecular oxygen into arachidonic acid to form the unstable intermediate PGG_2, which is rapidly converted into PGH_2 by the peroxidase activity of the same enzyme. Of the two COX isoforms, COX-1 is expressed constitutively in most tissues and is generally responsible for the production of PGs that control normal physiological functions, whereas COX-2 is inducible in response to mitogens, cytokines and cellular transformation. High levels of constitutive expression of COX-2 and its product PGE_2 have been detected in various cancer cells and tissues. Moreover, pharmacological, cell biological and gene targeting studies investigating COX-2 and EPs (PGE receptors) have demonstrated that PGE_2 produced through the COX-2-dependent pathway contributes to the progression of several types of cancer [4,5].

PGES catalyses the conversion of PGH_2, produced by COX-1 or COX-2, into PGE_2. Thus far, three PGES enzymes, mPGES (microsomal PGES)-1, mPGES-2 and cPGES (cytosolic PGES), have been identified [6–9]. Among these PGES isozymes, mPGES-1 is induced by pro-inflammatory stimuli and down-regulated by anti-inflammatory glucocorticoids, as in the case of COX-2, and is functionally coupled with COX-2 in marked preference to COX-1 [7,10,11]. Induction of mPGES-1 expression and its function have been observed in various diseases and systems in which COX-2-driven PGE_2 has been implicated, such as rheumatoid arthritis, febrile response, reproduction, bone metabolism, cardiovascular function, stroke and Alzheimer's disease [12,13]. Furthermore, it has previously been reported

Abbreviations used: COX, cyclo-oxygenase; cPGES, cytosolic prostaglandin E synthase; DMEM, Dulbecco's modified Eagle's medium; $dmPGE_2$, 16,16-dimethyl prostaglandin E_2; ECM, extracellular matrix; EP, prostaglandin E receptor; FCS, fetal calf serum; GAPDH, glyceraldehyde-3-phosphate dehydrogenase; HEK, human embryonic kidney; KD, knockdown; KO, knockout; LLC, Lewis lung carcinoma; MMP, matrix metalloproteinase; mPGES, microsomal prostaglandin E synthase; NSAID, non-steroidal anti-inflammatory drug; PG, prostaglandin; PGES, PGE synthase; RT, reverse transcriptase; siRNA, small interfering RNA; TBS, Tris-buffered saline; TBS-Tween, TBS containing 0.05% Tween 20; VEGF, vascular endothelial growth factor; WT, wild-type.

[1] To whom correspondence should be addressed (email haras@pharm.showa-u.ac.jp).

[2] Professor Kudo died on April 27, 2008. We greatly miss him as a scientist and a friend. We offer sincere thanks to all the friends, colleagues and former collaborators of Professor Kudo who showed him kindness during his lifetime.

that mPGES-1 is constitutively expressed in several cancers, most of which also express COX-2 constitutively [14,15]. We have reported that the forcible transfection of mPGES-1 in combination with COX-2, but not with COX-1, into HEK (human embryonic kidney)-293 cells led to cellular transformation with a concomitant and robust increase in PGE_2 [14]. Transgenic mice overexpressing both COX-2 and mPGES-1 developed metaplasia, hyperplasia and tumorous growth in the glandular stomach with heavy macrophage infiltration [16,17]. It has also been suggested that the PGE_2 produced through the COX-2-dependent pathway may regulate cancer–host communications that influence tumour progression. Studies using mice null for COX-2 or EPs have revealed that stromal cells around cancer cells express COX-2 and synthesize PGE_2, which, in tumour niches, may act on stromal cells in an autocrine fashion to induce the production of pro-angiogenic factors and consequent angiogenesis, as well as on cancer cells in a paracrine fashion to promote their growth, survival, adhesion and motility [5,18–20]. Although several studies, including our own, have found, by immunohistochemistry, that mPGES-1 is expressed in both stromal cells and cancer cells in tumour tissues [14,21], the contribution of mPGES-1 expressed in either cell population to tumour progression has not yet been fully elucidated.

Although the inhibition of COX-2-mediated PGE_2 formation represents a promising chemopreventive strategy for reducing the risk of cancer, the cardiovascular side effects associated with COX-2 inhibitors, which most likely result from the blunting of anti-thrombotic prostacyclin (PGI_2), have previously been found to limit their use [22,23]. From this viewpoint, selective blockage of the biosynthesis of PGE_2 without affecting other prostanoids appears to be feasible for cancer chemoprevention with the potential for improved tolerability over NSAIDs. To better evaluate the efficacy of mPGES-1 inhibition in relieving symptoms of cancer, the present study used lung carcinoma cells with mPGES-1 KD (knockdown) or overexpression, as well as mice null for mPGES-1. Our results provide evidence that mPGES-1 in both cancer cells and hosts contributes to tumorigenesis *in vitro* and *in vivo*.

EXPERIMENTAL

Cells

LLC (Lewis lung carcinoma) cells, which were originally isolated from C57BL/6 mice, were cultured in DMEM (Dulbecco's modified Eagle's medium) containing 10% (v/v) FCS (fetal calf serum) under a humidified atmosphere containing 5% CO_2. To establish mPGES-1-KD and -overexpressing LLC cells, we transfected these cells with a pRNA-U6.1/Hygro siRNA (small interfering RNA) expression vector (GenScript) harboring an mPGES-1-directed siRNA target sequence [5′-GGCCTTTGCCAACCCCGAG-3′ (residues 126–144 in the open reading frame)] and a pcDNA3.1 expression vector (Invitrogen) containing mouse mPGES-1 cDNA respectively, using Lipofectamine™ 2000 (Invitrogen). After the transfection of these plasmids, LLC cells were cultured in medium containing 1 mg/ml G418 (Invitrogen) to establish stable clones. As a control, LLC cells transfected with an empty vector (pRNA-U6.1/Hygro or pcDNA3.1) were used (referred to as mock cells hereafter).

Animals

C57BL/6 and BALB/c mice were obtained from the Saitama Animal Center. mPGES-1-KO (knockout) mice were established as described previously [12,13], and backcrossed at least three generations with C57BL/6 mice or ten generations with BALB/c mice. Female mPGES-1-KO mice and littermate WT (wild-type) mice (7-weeks-old) were used in each experiment. The mice were housed in microisolator cages in a pathogen-free barrier facility, and all procedures involving animals were performed in accordance with protocols approved by the Institutional Animal Care and Use Committee of Showa University, in accordance with the Standards Relating to the Care and Management of Experimental Animals in Japan.

Cell growth assay

Cells were seeded at 6×10^4 cells/well in six-well plates or 1.5×10^5 cells/flask in T-25 culture flasks in culture medium in the presence or absence of 10 nM NS-398 (Cayman Chemicals), a COX-2 selective inhibitor, or 1 mM dmPGE_2 (16,16-dimethyl PGE_2) (Cayman Chemicals), a metabolically stable analogue of PGE_2. After culture for 72 h, the cells were collected by trypsinization and counted in a Bright-line haemocytometer in the presence of Trypan Blue.

Western blot analysis

Aliquots of samples (20 μg of protein equivalents) were subjected to SDS/PAGE using 10% (w/v) gels under reducing conditions. The separated proteins were electroblotted on to nitrocellulose membranes (Schleicher & Schuell) with a semi-dry blotter (Bio-Rad). After blocking with 3% (w/v) dried non-fat skimmed milk in TBS (Tris-buffered saline) (pH 7.4) containing 0.05% Tween 20 (TBS-Tween), the membranes were probed with the respective antibodies for 2 h {1:2000 dilution for antibodies against mPGES-1 [14], mPGES-2 (Cayman Chemicals), cPGES [11], COX-1 and -2 (Santa Cruz Biotechnology), EP1, 2, 3 and 4 (Cayman Chemicals), and VEGF (vascular endothelial growth factor; Sigma); and 1:2500 dilution for anti-mouse α-tubulin antibody (Zymed Laboratories) in TBS-Tween}. After washing with TBS-Tween, the membranes were incubated with horseradish peroxidase-conjugated anti-goat (for COX-1, COX-2 and VEGF), anti-rabbit (for mPGES-1, mPGES-2, cPGES and EP1–4) and anti-mouse (for α-tubulin) IgG antibodies (1:5000 dilution in TBS-Tween) for 1 h, and visualized with the ECL (enhanced chemiluminescence) Western blot system (PerkinElmer Life Sciences), as described previously [7,13,14]. Amounts of individual proteins relative to that of α-tubulin were estimated from their signal intensities on the Western blots using Lane and Spot Analyzer (ATTO).

Determination of PG levels

For the measurement of PGs in tissues, mouse tissues were washed twice with Hank's balanced salt solution containing 10 μM indomethacin (Sigma) before homogenization. The supernatants obtained from the tissue homogenates were adjusted to pH 3.0 with 1 M HCl and passed through a Sep-Pak C_{18} cartridge (Waters), and the retained PGs were eluted with 8 ml of methanol, as described previously [13]. A trace amount of [^{3}H]PGE_2 (Cayman Chemicals) was added to the samples before passage through the cartridges to calibrate the recovery of the PGs. The sample solvents were evaporated, and then the PGs were dissolved in an aliquot of buffer and assayed with commercial enzyme immunoassay kits for individual PGs (Cayman Chemicals). Likewise, aliquots of the supernatants of cultured cells were subjected to the enzyme immunoassay for PGs.

Adhesion assay

Cells were plated at 2×10^5 cells in 35-mm dishes, which were pre-treated with collagen, fibronectin or laminin (BD Biosciences). After incubation for 60 min at 37 °C, the cells were fixed with Carnoy solution and then stained with Giemsa solution for 60 min. Adherent cells were counted in three fields at ×40 magnification using a microscope and J image software.

Invasion assay

Cell invasiveness was evaluated using a BD BioCoat™ Matrigel™ Invasion Chamber (BD Biosciences) according to the manufacturer's instructions. In brief, cells (1.2×10^6 cells in 0.5 ml) suspended in DMEM containing 3 % (v/v) FCS and 1 % (v/v) sodium pyruvate (Invitrogen) were seeded on the top of the gel in each chamber. DMEM containing 10 % (v/v) FCS (0.75 ml) was added as a source of chemoattractants into the bottom wells of the plate. After 16 h of incubation, cells that had invaded on to the lower surface of the chamber were fixed with methanol for 5 min, and stained with Crystal Violet. Non-invasive cells on the upper surface were removed with a cotton bud, and the membrane was cut. The number of invading cells was quantified by counting them under a light microscope. Statistical significance was determined using the Student's *t* test.

Tumour implantation model

LLC cells (1×10^6) in 100 μl of PBS were injected subcutaneously into 8-week-old female mice. Tumour growth was assessed by the measurement of two bisecting diameters in each tumour using calipers. The size of the tumour was determined by direct measurement of the tumour dimensions. The volume was calculated according to the equation: $V = (L \times W^2) \times 0.5$, where V = volume, L = length and W = width [35]. On day 14 after tumour implantation, the mice were anaesthetized and killed by dislocation of the cervical spine, and the tumour tissues were dissected, weighed and then fixed in 10 % (v/v) formalin for histochemical analyses. The intratumoral blood vessels in the most intensive neovascularization areas were quantified by staining of the sections with haematoxylin and eosin followed by silver. For each tumour, five random images were captured at ×400 magnification. Only areas of viable tumour tissue were imaged; necrotic regions were excluded. The individual microvessels were counted. The structure of individual microvessels was clearly differentiated from tumour cells on silver staining. The final vascular density score for the tumour represents an average of all scored fields.

Lung metastasis model

LLC cells (1×10^6) in 100 μl of PBS were intravenously injected into the lateral tail veins of 8-week-old female mice. Then, 14 days later, the mice were anaesthetized and killed, and the lungs were removed and weighed. Finally, the lungs were placed in Bouin's solution for 24 h and then photographed.

Determination of haemoglobin levels in tumour tissues

The dissected tumour tissues were washed, cut into small pieces with scissors, and homogenized with a Polytron homogenizer in a SET buffer [250 mM sucrose, 0.5 mM EDTA and 20 mM Tris/HCl (pH 7.4)] containing 10 μM indomethacin, 1 mM PMSF and 0.5 % Triton X-100. The tissue homogenates obtained were centrifuged at 600 *g* for 5 min, and an aliquot (200 μl) of the supernatant was centrifuged again at 14 000 *g* for 30 min at 4 °C. Concentrations of haemoglobin in the supernatant were then determined spectrophotometrically by measuring the absorbance at 540 nm using a haemoglobin assay kit (Wako).

RT (reverse transcriptase)–PCR

Total RNA was isolated from cells and tissues using TRIzol® (Invitrogen). Synthesis of cDNA was performed with 2 μg of the total RNA and avian myeloblastosis virus RT according to the manufacturer's instructions supplied with the RNA PCR kit version 2.1 (Takara Biomedicals). Subsequent amplifications of the partial cDNA fragments were performed using 0.5 μl of the reverse-transcribed mixture as a template with a set of specific oligonucleotide primers (Sigma) as follows: (i) mouse VEGF, sense 5′-GATGAAGCCCTGGAGTGC-3′ and antisense 5′-TCCCAGAAACAACCCTAA-3′; and (ii) mouse GAPDH (glyceraldehyde-3-phosphate dehydrogenase), sense 5′-TCGTGGATCTGACGTGCCGCCTG-3′ and antisense 5′-CACCACCCTBTTGCTGTAGCCGTAT-3′. The PCR mixtures were subjected to 30 cycles of amplification by denaturation (30 s at 94 °C), annealing (30 s at 57 °C) and elongation (30 s at 72 °C). The PCR products were analysed by 1 % (w/v) agarose gel electrophoresis with ethidium bromide.

Real-time RT–PCR

Single-stranded cDNA was generated using 1 μg of total RNA as a template and avian myeloblastosis virus RT, using a high capacity reverse transcriptase kit (Applied Biosystems). Real-time PCR was carried out using the SYBR Green PCR Master Mix (Applied Biosystems) and StepOne (Applied Biosystems) according to the manufacturer's instructions. The PCR primer sets used were: (i) mouse EP2, sense 5′-GCTGTGCTCGCCTGCAA-3′ and antisense 5′-CGACGGTGCATGCGAAT-3′; (ii) mouse EP4, sense 5′-CATCATCTGTGCCATGAGCAT-3′ and antisense 5′-GCTGTAGAAGTAGGCGTGGTTGA-3′; (iii) mouse VEGF, sense 5′-TACCTCCACCATGCCAAGTG-3′ and antisense 5′-TGGGACTTCTGCTCTCCTTCTG-3′; (iv) mouse MMP (matrix metalloproteinase)-2, sense 5′-GGACCCCGGTTTCCCTAA-3′ and antisense 5′-CAGGTTATCAGGGATGGCATTC-3′; (v) mouse MMP-9, sense 5′-AGTGGGACCATCATAACATCACAT-3′ and antisense 5′-TCTCGCGGCAAGTCTTCAG-3′; (vi) mouse α5 integrin, sense 5′-ATGGCTCAGACATCCACTCC-3′ and antisense 5′-GGTCATCTAGCCCATCTCCA-3′; and (vii) mouse β1 integrin, sense 5′-GGTGTCGTGTTTGTGAATGC-3′ and antisense 5′-TGACGCTAGACATGGACCAG-3′. The expression levels of EP2, EP4, MMP-2, MMP-9 and integrins were normalized with those of mouse GAPDH with a primer set of 5′-ATGTGTCCGTCGTGGATCTGA-3′ and 5′-ATGCCTGCTTCACCACCTTCT-3′. Results represent an average of several independent experiments.

Gelatin zymography

Lysates of cells and tissues (27 μg of protein equivalents) were subjected to SDS/PAGE (10 % gels), with 1 mg/ml gelatin substrate being incorporated into the gels. Following electrophoresis, the gels were soaked in 2.5 % Triton X-100 to remove SDS, rinsed with 10 mM Tris/HCl (pH 8.0), and transferred to a bath containing 50 mM Tris/HCl(pH 8.0), 5 mM $CaCl_2$ and 1 μM $ZnCl_2$ at 37 °C for 18 h. The gels were then stained with 0.1 % Coomassie Blue in 45 % methanol and 10 % acetic acid.

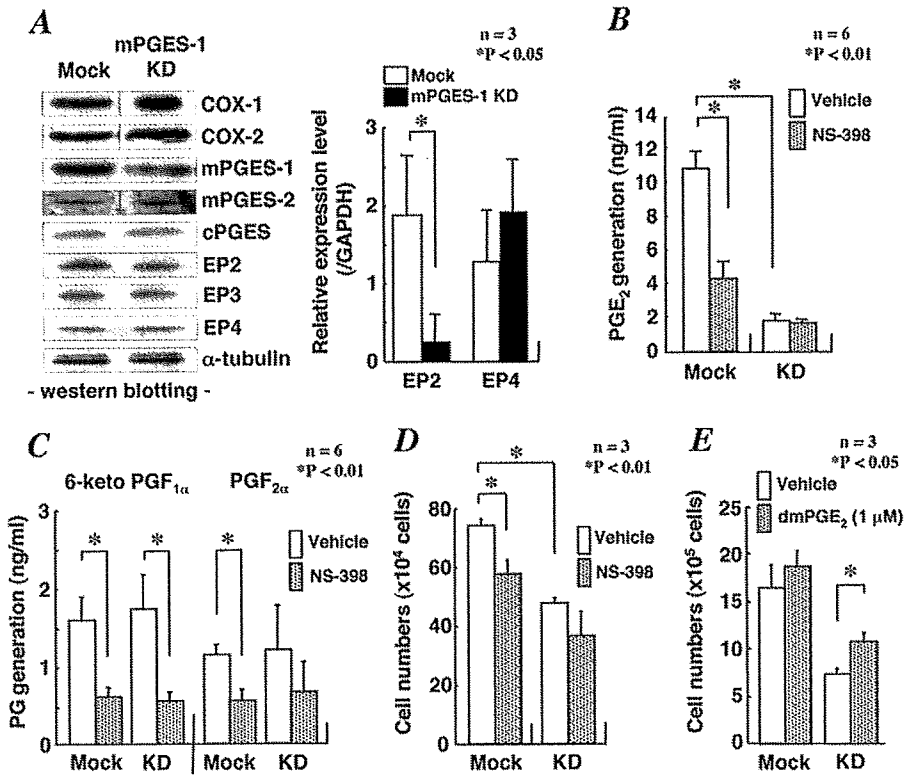

Figure 1 PGE_2 production and cell proliferation in mPGES-1-silenced LLC cells *in vitro*

(**A**) Expression of PGE_2 biosynthetic enzymes and PGE receptors in mPGES-1-KD and control (mock) cells was assessed by immunoblotting (left-hand panel). Equal amounts of cell lysates (20 μg of protein equivalents) were separated by SDS/PAGE and analysed by Western blotting at the same time with the corresponding antibodies to allow for a direct comparison. Representative results of at least three experiments are shown. Expression levels of EP2 and EP4 mRNAs in KD and mock cells were evaluated by quantitative RT–PCR, with GAPDH mRNA used for normalization (right-hand panel). (**B–D**) Effects of mPGES-1 silencing and 10 nM NS-398, a COX-2 selective inhibitor, on production of PGE_2 (**B**), 6-keto $PGF_{1\alpha}$ and $PGF_{2\alpha}$ (**C**), and on cell proliferation (**D**). mPGES-1-KD and mock cells were seeded at 6×10^4 cells/well in six-well culture dishes in the presence or absence of 10 nM NS-398. After culture for 3 days, the cells were collected and counted in a Bright-line haemocytometer in the presence of Trypan Blue, and the supernatants were taken for enzyme immunoassay of several PGs. (**E**) Effect of $dmPGE_2$ on cell proliferation. mPGES-1-KD and mock cells were seeded in T-25 culture flasks at 1.5×10^5 cells/flask in culture medium in the presence or absence of 1 μM $dmPGE_2$. After culture for 3 days, the cells were collected and counted. Values are the means $\pm$ S.E.M. Similar results were obtained in three independent cell lines of mPGES-1-KD and control cells.

RESULTS

Reduced tumorigenic potential of mPGES-1-silenced LLC cells *in vitro*

We established mPGES-1-KD LLC cells by means of an siRNA-silencing strategy, as described in the Experimental section. The expression levels of mPGES-1 and other enzymes involved in PGE_2 synthesis in mPGES-1-KD and mock cells were examined by Western blot analysis (Figure 1A). The expression level of mPGES-1 was reduced by ~80% in mPGES-1-KD cells relative to mock cells, whereas those of COX-1 and -2 and other PGE synthases (cPGES and mPGES-2) in both cell lines were approximately the same (Figure 1A, left-hand panel). Furthermore, we found that, among the four EP receptor subtypes that can bind to PGE_2 [24], LLC cells expressed detectable levels of EP2, EP3 and EP4 proteins, among which the level of EP2 protein was reduced in mPGES-1-KD cells relative to mock cells, whereas the levels of EP3 and EP4 were unaffected by mPGES-1 silencing (Figure 1A, left-hand panel). The reduction in EP2, but not EP4, expression in the KD cells was verified by quantitative RT–PCR (Figure 1A, right-hand panel) and quantifying individual immunoblots by a densitometer (Supplementary Figure S1 at http://www.BiochemJ.org/bj/425/bj4250361add.htm). The amounts of PGE_2 released into the medium during culture were decreased in mPGES-1-KD cells relative to mock cells (Figure 1B), whereas those of 6-keto $PGF_{1\alpha}$ (a non-enzymatic hydrolytic product of PGI_2) and $PGF_{2\alpha}$ were comparable between mPGES-1-KD cells and mock cells (Figure 1C).

Concurrently, mPGES-1-KD cells grew more slowly than did mock cells (Figure 1D). NS-398, a COX-2-selective inhibitor, suppressed PGE_2 generation and cell proliferation in mock cells by ~60% and ~25% respectively, whereas no further decreases in PGE_2 production and cell growth were found in mPGES-1-KD cells (Figures 1B and 1D). Production of 6-keto $PGF_{1\alpha}$ and $PGF_{2\alpha}$ was equally sensitive to NS-398 in both cell lines (Figure 1C). Furthermore, cell growth of mPGES-1-KD cells was partially (even if not completely, probably because EP2 expression was reduced in the KD cells; see above) restored by addition of an optimal concentration (1 μM) of $dmPGE_2$, a synthetic analogue of PGE_2 (Figure 1E). These results suggest that the PGE_2 produced through the COX-2/mPGES-1 pathway is partially required for the proliferation of LLC cells.

In the process of tumour metastasis, cancer cells from the primary tumour must invade the ECM (extracellular matrix). There are many reports demonstrating that malignant tumour cells often possess high invasive activity [25]. Thus we next assessed the effect of mPGES-1 silencing on the invasive activity of LLC cells using Matrigel™ invasion chambers. As shown in Figure 2(A), the number of mPGES-1-KD cells migrating across the Matrigel™-coated filter was markedly fewer than that of mock cells. Since it is known that the PGE_2 signalling activates the invasive potential of cancer cells by increasing the expressions

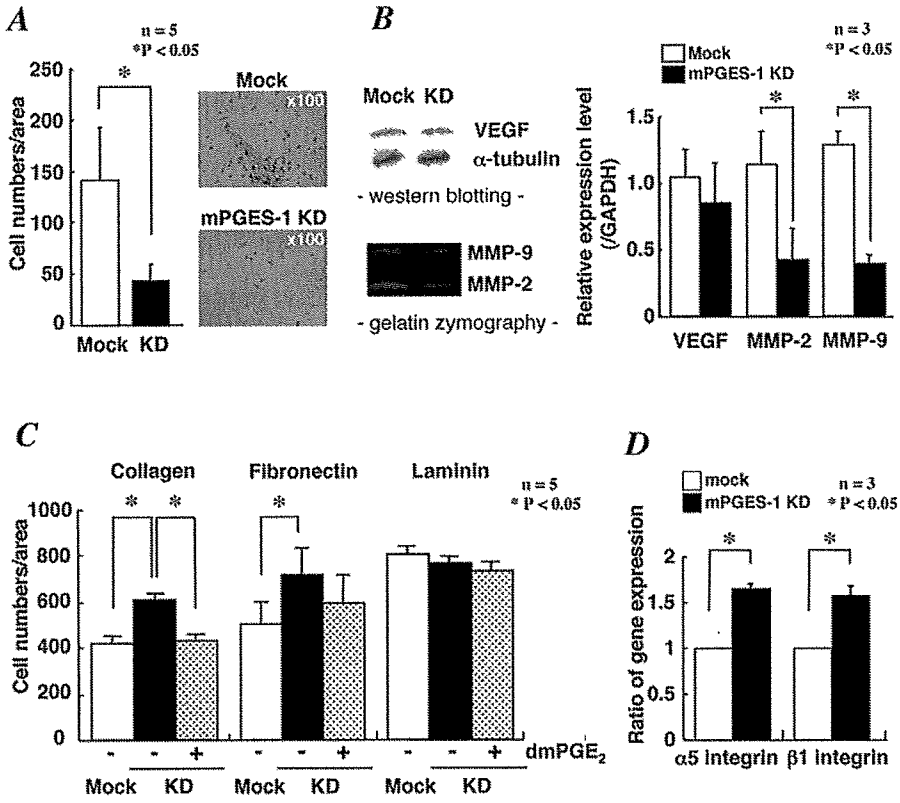

Figure 2 siRNA silencing of mPGES-1 in LLC cells reduces their malignant potential *in vitro*

(**A**) mPGES-1-KD and mock cells [1.2 × 10^6 cells in DMEM containing 3% (v/v) FCS] were seeded on to the upper wells of BD BioCoat™ Matrigel™ Invasion Chambers. DMEM containing 10% (v/v) FCS was added as a source of chemoattractants into the bottom wells of the plates. After 16 h of incubation, cells that had invaded on to the lower surface of the chambers were fixed, stained with Crystal Violet and counted (left-hand panel). Values are the means ± S.E.M. of five independent experiments. Representative photographs of mPGES-1-KD and mock cells that invaded across the Matrigel™-coated inserts are shown (right-hand panel). (**B**) The expression of VEGF protein in mPGES-1-KD and mock cells was assessed by immunoblotting (upper panel). The cell lysates (20 μg of protein equivalents) were separated by SDS/PAGE and then subjected to Western blot analysis using anti-VEGF and anti-α-tubulin antibodies. The activities of MMP-2 and -9 in mPGES-1-KD and mock cells were assessed by gelatin zymography (lower panel). Lysates of cells (27 μg of protein equivalents) were subjected to SDS/PAGE containing 1 mg/ml gelatin. Following electrophoresis, the gels were incubated in a bath containing 1 μM $ZnCl_2$ at 37°C for 18 h. The gels were then stained with 0.1% Coomassie Blue. The expression levels of mRNAs for VEGF, MMP-2 and MMP-9 were evaluated by quantitative RT–PCR, with GAPDH mRNA used for normalization (means ± S.D.; $n = 3$) (right-hand panel). (**C**) Adhesion of mPGES-1-KD and mock cells to ECM proteins. mPGES-1-KD or mock cells (2 × 10^5 cells) were seeded on to 35-mm dishes coated with collagen, fibronectin or laminin in culture medium in the presence or absence of 1 μM $dmPGE_2$. After allowing cells to attach for 60 min at 37°C, non-adherent cells were removed by washing. Adherent cells were fixed and stained with Giemsa solution and counted in three fields at ×40 magnification using a microscope and J image software. Values are the means ± S.E.M. of five independent experiments. (**D**) Expression of α5 and β1 integrins in mPGES-1-KD and mock cells. Total RNA was isolated from mPGES-1-KD and mock cells and subjected to quantitative RT–PCR using specific primers of α5 (left-hand panel) and β1 (right-hand panel) integrins and those of GAPDH as a reference. The results of quantitative RT–PCR were normalized with their expression in mock cells being regarded as 1 (means ± S.D., $n = 3$). Similar results were obtained in two independent cell lines of mPGES-1-KD and control cells.

of VEGF, a pro-angiogenic factor, and MMPs, which hydrolyse type IV collagen localized in the basement membrane [25], we next examined the effects of mPGES-1 silencing on the expression of VEGF and the activities of MMP-2 and -9 by Western blot analysis, gelatin zymography and quantitative RT–PCR. As shown in Figure 2(B), the activities of MMP-2 and -9 in the conditioned medium from mPGES-1-KD cells were lower than those in the medium from mock cells. Consistently, expression levels of both MMP-2 and -9 mRNAs were significantly reduced in the KD cells relative to control cells. In contrast, the levels of VEGF protein and mRNA were unaffected by mPGES-1 silencing (Figure 2B). These results suggest that the silencing of mPGES-1 diminishes *in vitro* migration of LLC cells by reducing the PGE_2-induced expression of MMP-2 and -9.

The ability of cancer cells to adhere to the ECM influences their motility and invasion in tumour tissues *in vivo*, and metastatic tumour cells show decreased ECM-adherent activity *in vitro* [25,26]. Therefore we next studied the attachment of mPGES-1-KD or mock cells to culture dishes pre-coated with distinct ECM components. The results showed that the numbers of mPGES-1-KD cells adhering to collagen and fibronectin, but not to laminin, were significantly increased as compared with those of mock cells (Figure 2C). Moreover, the increased adhesion of mPGES-1-KD cells to collagen was reversed by $dmPGE_2$ to the level of mock cells, and adhesion of the cells to fibronection also showed a similar trend (Figure 2C). Consistent with the increased binding of mPGES-1-KD cells to collagen and fibronectin, the expressions of their receptor components, α5 and β1 integrins, were elevated in the KD cells relative to control cells (Figure 2D). Thus we conclude that mPGES-1 supplies a majority of the PGE_2 that enhances the malignant potential (in terms of ECM invasion and adherence) of cancer cells.

Increased tumorigenic potential of mPGES-1-overexpressing LLC cells *in vitro*

We next established LLC cells that stably overexpressed mPGES-1 and examined whether these cells (as opposed to

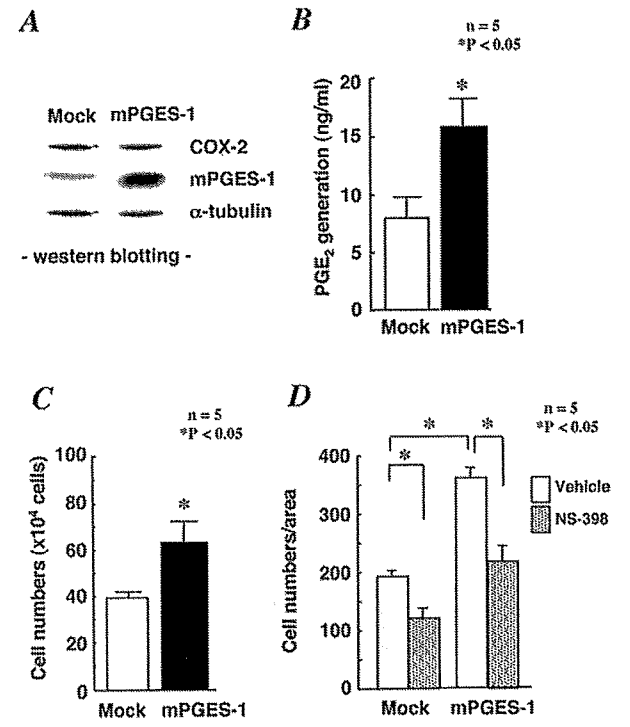

Figure 3 Increased PGE_2 generation, proliferation and invasion of mPGES-1-overexpressing LLC cells

(**A**) Expression of COX-2 and mPGES-1 in mPGES-1-overexpressing and mock cells was assessed by Western blot analysis. Representative results of at least three experiments are shown. (**B** and **C**) Effects of mPGES-1 overexpression on PGE_2 generation (**B**) and cell growth (**C**). mPGES-1-overexpressing and mock cells were seeded at 6×10^4 cells/well in six-well culture dishes. After culture for 2 days, the cells were collected and counted, and the supernatants were taken for a PGE_2 enzyme immunoassay. Values are the means ± S.E.M. of five independent experiments. (**D**) mPGES-1-overexpressing and mock cells (1.2×10^6 cells in the presence or absence of 10 nM NS-398) that had invaded through BD BioCoat™ Matrigel™ Invasion Chamber inserts over 16 h were counted. Values are the means ± S.E.M. of five independent experiments. Similar results were obtained in two independent cell lines of mPGES-1-overexpressing and mock cells.

mPGES-1-KD cells) would show increased proliferation and invasion. mPGES-1-transfected LLC cells expressed more mPGES-1 protein than did mock cells, whereas the expression of COX-2 protein was unaltered (Figure 3A). PGE_2 release into the medium during culture was increased by ~2-fold in mPGES-1-overexpressing cells relative to mock cells (Figure 3B). As shown in Figure 3(C), the growth rate of mPGES-1-overexpressing cells was significantly faster than that of mock cells. Moreover, the Matrigel™ invasion chamber assay revealed that the invasive activity of mPGES-1-overexpressing cells was notably higher than that of mock cells (Figure 3D). Additionally, treatment of both mock and mPGES-1-overexpressing LLC cells with NS-398 reduced the invasion by ~40% (Figure 3D). These results confirm that the increased production of PGE_2 through the COX-2/mPGES-1 pathway in cancer cells facilitates their proliferation and invasion.

Silencing of mPGES-1 in cancer cells reduces tumorigenesis *in vivo*

To assess the contribution of mPGES-1 in cancer cells to tumour development *in vivo*, we grafted mPGES-1-KD and mock LLC cells subcutaneously into BALB/c mice, and the development of the solid tumour around the injection sites was evaluated on day 14 after implantation. Remarkably, both the volume and mass of xenografts derived from mPGES-1-KD cells were significantly smaller than those derived from mock cells (Figures 4A and 4B). The levels of prostanoids (PGE_2, $PGF_{2\alpha}$ and 6-keto-$PGF_{1\alpha}$) in the homogenates of xenografts did not differ significantly between the genotypes, even though PGE_2 tended to decrease in the xenografts from mPGES-1-KD cells compared with those from mock cells (Figure 4C). The expression of VEGF, as assessed by RT–PCR and quantitative RT–PCR, was reduced in mPGES-1-KD xenografts as compared with control xenografts (Figure 4D). Considering that VEGF expression was unaltered by silencing of mPGES-1 in LLC cells *in vitro* (Figure 2B), the reduction of VEGF expression in mPGES-KD xenografts *in vivo* may reflect the action of mPGES-1-derived PGE_2 from cancer cells on proximal stromal cells in tumour microenvironments.

Reduced tumour growth and angiogenesis in mPGES-1-KO mice

The observations described above indicate that cancer cell-associated COX-2 and mPGES-1 co-operatively produce PGE_2, which accelerate multiple steps of malignant progression, including cell proliferation, invasion and ECM adhesion. In terms of the pathological circumstances, it has been reported that COX-2 and mPGES-1 are expressed not only in tumour cells, but also in the stromal cells (mainly in infiltrating macrophages) surrounding them [14,21]. To investigate the contribution of host-associated mPGES-1 to tumour growth, we next grafted parental LLC cells subcutaneously into either mPGES-1-KO or WT mice, and evaluated the development of solid tumour around the injection sites. Although the absence of mPGES-1 in the host mice influenced neither the engraftment rate nor the growth of tumours during the first 5 days after implantation, tumours grafted into the mPGES-1-KO mice were significantly smaller in size than those grafted into the WT mice after day 6 and beyond (Figure 5A). On day 14 after implantation, the tumour mass in mPGES-1-KO mice was reduced to half of that in WT mice (Figure 5B, left-hand panel). The levels of PGE_2 in homogenates of the dissected tumour tissues were nearly 50% less in mPGES-1-KO mice than in WT mice, whereas those of $PGF_{2\alpha}$ were unaffected by the host mPGES-1 deficiency (Figure 5B, right-hand panel).

Histological examination of the xenografts revealed that the vascularization of tumour tissues was markedly reduced by the lack of host mPGES-1 expression (Figure 5C, indicated by arrowheads). The vascular density was approx. 60% lower in tumours grafted in mPGES-1-KO mice than those grafted in WT mice (Figure 5D, left-hand panel). The haemoglobin contents in the tumour tissues, which appeared to be well correlated with tumour neovascularization upon histological examination [30], were also reduced in mPGES-1-KO mice in comparison with that in WT mice (Figure 5D, right-hand panel). The reduction of tumour angiogenesis in mPGES-1-KO mice caused a large area of central necrosis in the xenografts of mPGES-1-KO, but not WT, mice (Figure 5C, indicated by an asterisk). We further found that the expression levels of the VEGF protein and mRNA in tumour tissues were also markedly lower in mPGES-1-KO mice than in WT mice (Figure 5E, left-hand panel). The decrease in VEGF protein in the xenografts of mPGES-1-KO mice was confirmed by quantification of the relative abundance of VEGF to α-tubulin using a densitometer (Figure 5E, right-hand panel). These results suggest that host mPGES-1-derived PGE_2 plays a pivotal role in tumour-associated VEGF production and accompanying angiogenesis. Again, considering that VEGF expression was

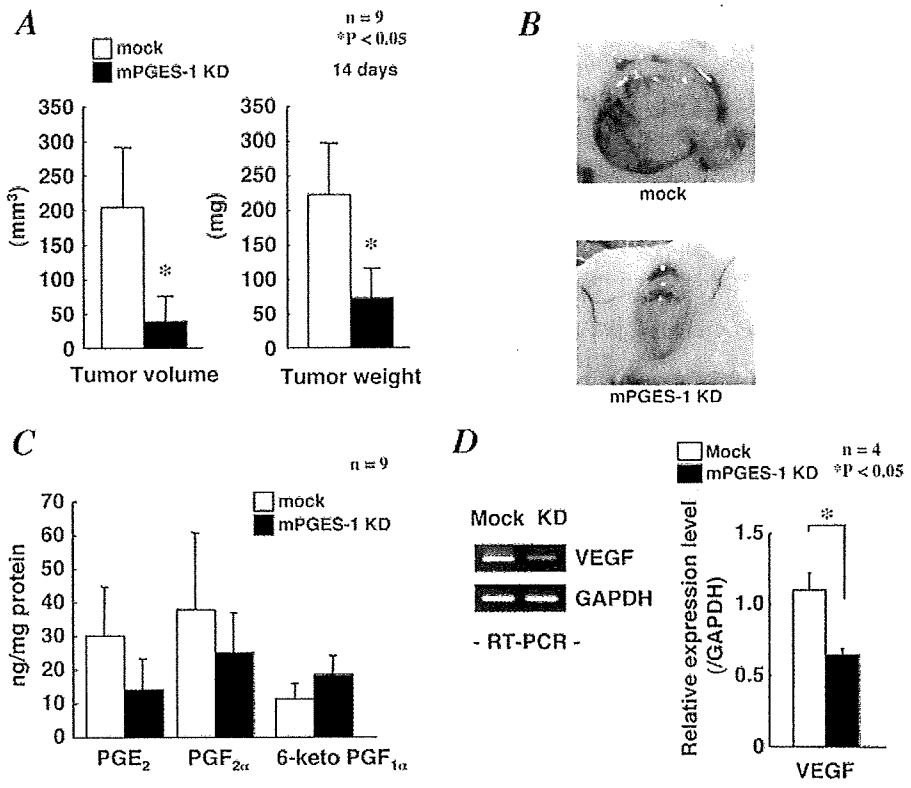

Figure 4 siRNA silencing of mPGES-1 in cancer cells reduces tumorigenesis *in vivo*

(**A–C**) mPGES-1-KD or mock cells (10^6 cells) were injected into the subcutaneous tissue of female BALB/c mice. On day 14 after implantation, tumour volume was scored according to the formula $V = (L \times W^2) \times 0.5$ (**A**, left-hand panel). The tumour tissues were photographed at × 100 magnification (**B**), dissected and weighed (**A**, right-hand panel). Values are means ± S.E.M. ($n = 9$). (**C**) Amounts of PGE_2, $PGF_{2\alpha}$ and 6-keto $PGF_{1\alpha}$ in homogenates of the tumour tissues were quantified by enzyme immunoassay (means ± S.E.M., $n = 9$). (**D**) Expression of VEGF in tumour xenografts of mPGES-1-KD and mock cells was assessed by RT–PCR followed by electrophoresis (left-hand panel) and quantitative RT–PCR (right-hand panel), with the expression of GAPDH as a reference (means ± S.D., $n = 4$).

unaltered in mPGES-1-KD cells *in vitro* (Figure 2B), the reduced expression of this angiogenic factor in tumour tissue in mPGES-1-KO mice may reflect the impact of mPGES-1-derived PGE_2 on tumour microenvironments rather than on tumour cells *in vivo*.

We further examined the role of host-associated mPGES-1 in tumour metastasis by intravenous injection of parental LLC cells into mPGES-1-KO and WT mice. After 14 days, macroscopic metastases, as assessed by Bouin's staining, were found in the lungs of both genotypes, but the number and size of metastatic foci (Figure 6A) and the mass (Figure 6B, left-hand panel) of the lungs were significantly reduced in mPGES-1-KO mice compared with WT mice. Levels of PGE_2 were reduced by nearly 50% in homogenates of the lungs from mPGES-1-KO mice relative to WT mice (Figure 6B, right-hand panel). Moreover, as assessed by RT–PCR and quantitative RT–PCR, VEGF expression in the metastasized lungs was significantly lower in mPGES-1-KO mice than in WT mice (Figures 6C and 6E). Gelatin zymography revealed that the activity of MMP-2 in the metastasized lung tissues was mitigated in mPGES-1-KO mice in comparison with that in WT mice (Figure 6D), and the levels of both MMP-2 and -9 mRNAs were significantly lower in the lung of mPGES-1-KD mice than in that of WT mice (Figure 6E). Collectively, these results indicate that host mPGES-1-driven PGE_2 plays a role in promoting tumour development and metastasis, which was associated with increased VEGF expression and MMP-2 and -9 activation.

DISCUSSION

Although the concept that the PGE_2 produced through the COX-2-dependent pathway participates in the pathogenesis of several types of cancer has been well established in the past decade based on a series of genetic studies employing mice ablated for the biosynthetic enzymes (COX-2) and receptors (EPs) or pharmacological studies employing inhibitors or agonists/antagonists fairly specific for them, the contribution of a step between COX-2 and EPs, namely PGES enzymes that convert COX-2-produced PGH_2 into PGE_2, to cancer development has remained incompletely understood. In this context, we have previously shown that co-transfection of mPGES-1 in combination with COX-2 into HEK-293 cells leads to a malignant phenotype [14]. In our continuing efforts to gain further insights into the role of mPGES-1 in tumorigenesis, we used two approaches in the present study. First, we performed siRNA-mediated silencing and overexpression of mPGES-1, which enabled us to address the complementary effects of endogenous compared with overexpressed mPGES-1 in cancer cells on tumorigenic potentials (growth, invasion and ECM binding *in vitro* and tumour xenograft propagation *in vivo*). Secondly, implantation of carcinoma cells into mPGES-1-KO mice and WT mice allowed us to evaluate the contribution of mPGES-1 expressed in tissue microenvironments to the development and metastasis of tumours in proximal and distant tissues. Our results clearly indicate that mPGES-1 expressed in both cancer cells and

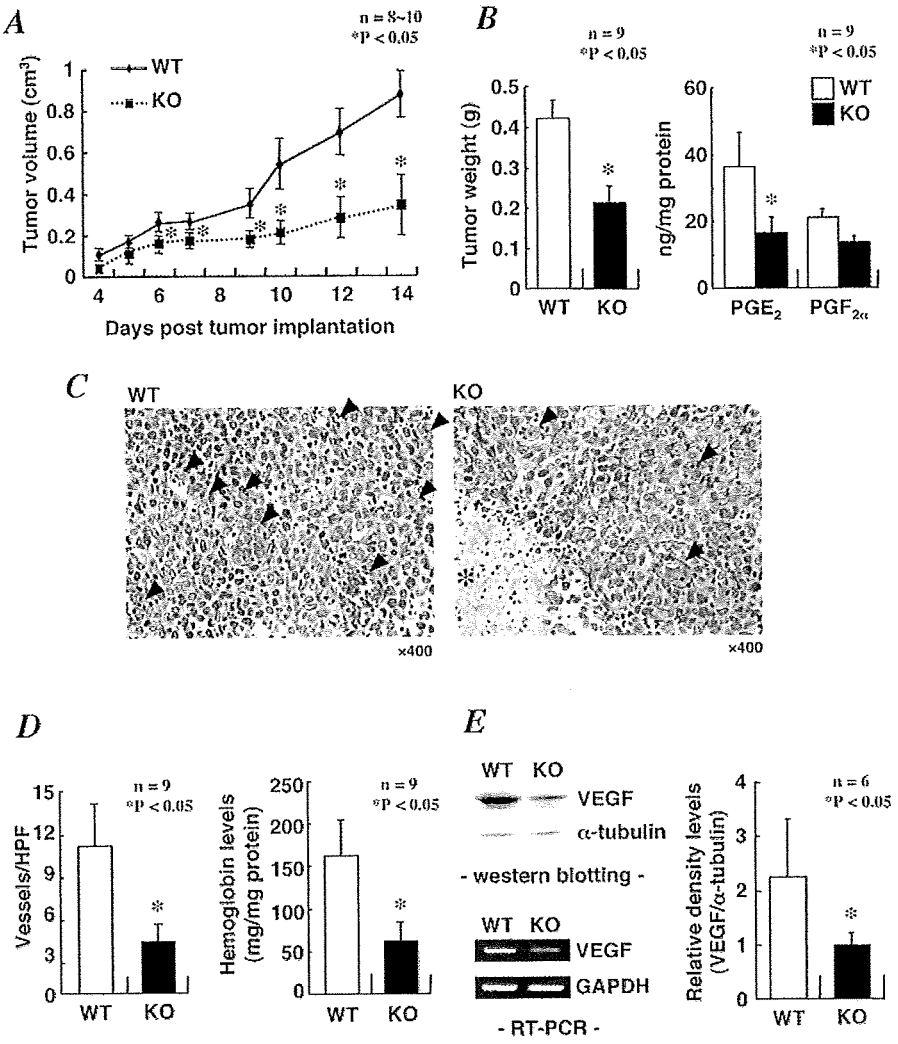

Figure 5 Growth of LLC cells subcutaneously implanted into mPGES-1-KO and WT mice

A total of 10^5 cells were injected into the subcutaneous tissue of female mPGES-1-KO and WT mice. (**A**) Tumour volumes were scored on the indicated days as described in the Experimental section. (**B**) On day 14 after implantation, the tumour tissues were dissected and weighed (left-hand panel). Amounts of PGE_2 and $PGF_{2\alpha}$ in homogenates of the tumour tissues were quantified by enzyme immunoassay (right-hand panel). Results are presented as the means ± S.E.M. ($n = 9$). (**C**) Tumour tissues were cut out, fixed in formalin, and stained with silver, haematoxylin and eosin for histochemical analysis. Microvessels and necrotic regions are shown by arrowheads and an asterisk respectively. (**D**) Vascular density (left-hand panel) and haemoglobin content (right-hand panel) were determined as described in the Experimental section. Results are presented as the means ± S.E.M. ($n = 9$). HPF, high-power field. (**E**) Expression levels of VEGF protein (upper panel) and mRNA (lower panel) in the tumour tissues were determined by Western blot and RT–PCR analysis respectively. Representative results of six independent experiments are shown. On Western blot analysis, the expression level of VEGF protein was quantified by a densitometer, with the expression level of α-tubulin used for normalization (means ± S.D., $n = 6$) (right-hand panel).

hosts is capable of promoting proliferation and invasion of cancer cells *in vitro* and *in vivo*.

Role of mPGES-1 in cancer cells

We found that PGE_2 generation and cell proliferation were reduced by mPGES-1 knockdown (Figures 1A, 1B and 1D) and conversely enhanced by mPGES-1 overexpression (Figures 3A–3C) in LLC cells (a PGE_2-dependent mouse lung carcinoma cell line; [27]), indicating the role of mPGES-1, acting downstream of COX-2, in providing the mitogenic PGE_2. In accordance with the impact on cell proliferation, the gene silencing of mPGES-1 decreased, whereas overexpression of mPGES-1 increased, the invasive activity of LLC cells (Figures 2A and 3D). The process by which tumour cells break out from their site of origin and metastasize to distant sites requires an ability to invade through the ECM and underlying mesenchymal cells. PGE_2 stimulates the invasion of cancer cells through up-regulating MMP-2 and MMP-9 (type IV collagenases), as shown by the observations that MMP-2 is increased in COX-2-overexpressing or PGE_2-treated tumour cells [25,26,28,29], and that MMP-9 is induced by COX-2/EP4 signalling in macrophages [30]. We found that the expression of MMP-2 and -9 in mPGES-1-KD cells were lower than that in mock cells (Figure 2B), suggesting the contribution of these matrix-degrading proteases to the mPGES-1-dependent invasiveness of LLC cells. In addition to adhesion to and degradation of the ECM, detachment from the ECM is also an important step in the metastasis of tumour cells [25,26]. As shown in Figure 2(C), both collagen- and fibronectin-adherent activities were significantly increased in mPGES-1-KD cells, and treatment with $dmPGE_2$ reversed these activities consistently. Accordingly, the expression of integrin $\alpha 5\beta 1$ (a major adhesion molecule of fibronectin) in mPGES-1-KD cells was higher than that in

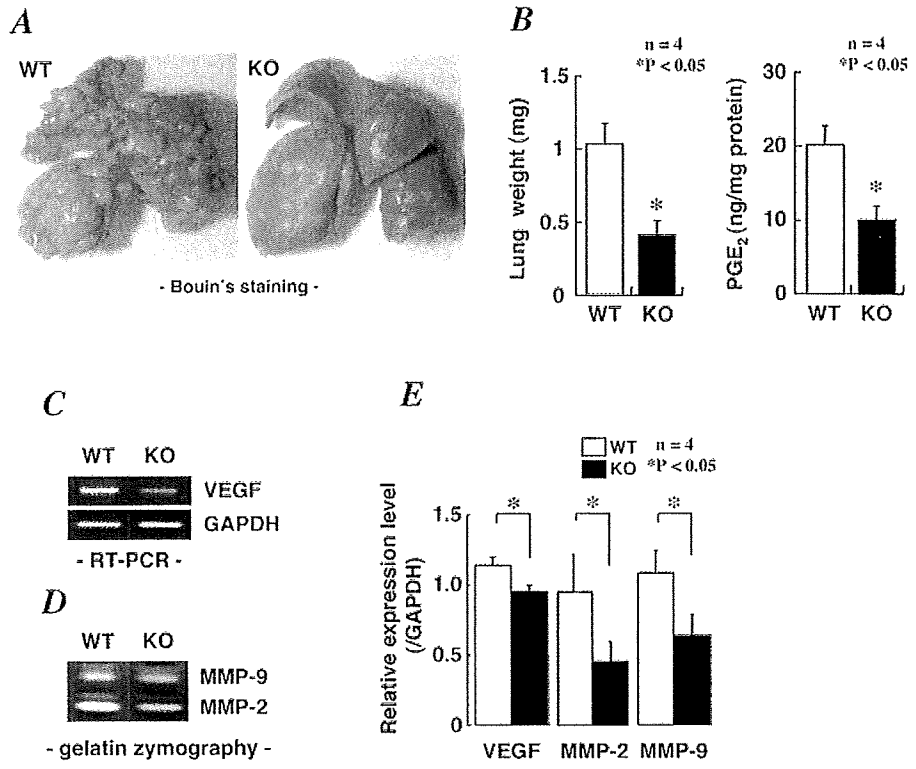

Figure 6 Reduced lung metastasis in mPGES-1-KO mice

A total of 10^5 cells were injected into the lateral tail veins of female mPGES-1-KO and WT mice on the BALB/c background. On day 14 after implantation, the mice were killed, and the removed lungs were weighed (**B**, left-hand panel) and then stained with Bouin's solution (**A**). Amounts of PGE_2 in homogenates of the metastasized lung tissues were measured by enzyme immunoassay (**B**, right-hand panel). (**C**) Expression of VEGF and GAPDH mRNAs were assessed by RT–PCR. (**D**) Activities of MMP-2 and -9 were evaluated by gelatin zymography. Results are presented as the means ± S.E.M. ($n = 4$) in (**B**) and representative results of four independent experiments are shown in (**A**, **C** and **D**). (**E**) The expression levels of mRNAs for VEGF, MMP-2 and MMP-9 were evaluated by quantitative RT–PCR, with GAPDH mRNA used for normalization (means ± S.D., $n = 4$).

mock cells (Figure 2D), an observation that is reminiscent of our previous report that co-overexpression of COX-2 and mPGES-1 in HEK-293 cells results in a marked reduction in a subset of integrins [14]. Thus mPGES-1-driven PGE_2 may regulate the ECM-adherent activity of cancer cells by altering the expression of integrins.

Importantly, *in vivo* tumour growth after subcutaneous engraftment of mPGES-1-KD cells was less obvious than that after engraftment of replicate mock cells (Figure 4), implying that mPGES-1 contributes to the supply of the major pool of the PGE_2 mediating tumour proliferation both *in vitro* and *in vivo*. Gene disruption of EP2 resulted in a reduced number and size of intestinal polyps in *Apc*-mutant mice, a model for human familial adenomatous polyposis [31], and the *Apc* mutation is accompanied by aberrant activation of β-catenin signalling, which is accelerated by PGE_2 through the EP2–Gsα axis [32,33]. In another model, disruption of the gene for EP1, EP2 or EP4 suppressed the development of colorectal cancer induced by carcinogens [34–36]. Transactivation of EGF (epidermal growth factor) receptors by the PGE_2/EP1, 2, or 4 signalling via protein kinase A and c-Src led to increased cell growth and invasion of carcinoma cells [37–39]. In a positive-feedback loop, COX-2-derived PGE_2 acts on EP2, leading to the elevation of intracellular cAMP, which in turn up-regulates the expressions of both COX-2 and EP2 [40]. Although the identification of EPs participating in the propagation of LLC xenografts is beyond the scope of the present study, the co-ordinated reduction of mPGES-1 and EP2 in mPGES-1-KD cells (Figure 1A) suggests that COX-2/mPGES-1-derived PGE_2 may stimulate EP2 signalling in an autocrine/paracrine fashion to facilitate LLC cell proliferation and, accordingly, defects in mPGES-1 may lead to down-regulation of EP2 and eventually reduce the cellular sensitivity to PGE_2.

While this paper was in preparation, two groups reported opposite effects of mPGES-1 deficiency in intestinal tumorigenesis. Nakanishi et al. [41] showed that the genetic deletion of mPGES-1 ameliorates the development of intestinal tumours in both $Apc^{\Delta 14}$-dependent and carcinogen-induced models, whereas Elander et al. [42] demonstrated that intestinal polyposis is exacerbated in mPGES-1-null Apc^{min} mutant mice, probably because of the metabolic shift from PGE_2 towards other pro-tumorigenic lipid mediators. Although the reason for the discrepancy between these two studies is unclear, our present results appear to be in line with the former study and thus support the feasibility of targeting mPGES-1 for cancer chemoprevention. Critically, although the experimental design of the previous studies did not allow a precise distinction between the contribution of cancer cell- and host-associated mPGES-1 to tumour development, our present approach clearly underscores the importance of mPGES-1 pools both in cancer cells (as discussed above) and in microenvironments (see below).

Role of mPGES-1 in host microenvironments

As is COX-2, mPGES-1 is expressed in stromal cells as well as in cancerous cells in several types of tumour [14,15]. Given that stromal COX-2 and PGE_2 of the host can influence the

development of grafted tumours [20,43], we used mPGES-1-KO mice to evaluate the potential roles of the host stromal mPGES-1 in tumour growth, and found that tumour growth at a proximal site and metastasis into a distant tissue were significantly reduced in mPGES-1-KO mice relative to WT mice (Figures 5 and 6). This result provides an additional line of genetic evidence that the COX-2/mPGES-1-derived PGE_2 from host stromal cells, in addition to that from cancer cells (see above), is important for tumorigenesis *in vivo*. The induction of mPGES-1 in tumour stromal tissues may be ascribed to the migration and expansion of host inflammatory cells and neovascular endothelial cells, since previous immunohistochemical analyses have demonstrated a preferential localization of mPGES-1 in macrophage-like cells infiltrating into the stromal tissues in proximity to cancer cells [14], and since massive macrophage infiltration and microvessel formation have been observed in the stroma of gastric hyperplasia in COX-2/mPGES-1-double transgenic mice [16,17].

As shown in Figure 5, vascular density and VEGF expression in tumour xenografts were decreased in mPGES-1-KO mice. It has been reported that angiogenesis induced by either endogenous COX-2 or exogenous PGE_2 was accompanied by increased VEGF expression and was abolished by a VEGF-directed antisense oligonucleotide [19]. Moreover, the growth, VEGF expression and angiogenesis of LLC-implanted tumours were markedly suppressed in EP3-KO mice [43], a phenotype that is reminiscent of mPGES-1-KO (the present study) and COX-2-KO mice [20]. These studies indicate that, in the tumour milieu, both cancer cells and adjacent stromal cells synthesize (via COX-2/mPGES-1) PGE_2, which in turn acts on the particular population of EP3-expressing stromal cells to induce the production of VEGF and consequent angiogenesis [43]. Consistently, Nakanishi et al. [41] have reported very recently that genetic deletion of mPGES-1 in *Apc*-mutant mice caused marked and persistent suppression of intestinal cancer growth in association with a disorganized vascular pattern. In addition to tumour growth and associated angiogenesis, lung metastasis of LLC cells across the blood circulation was also decreased in mPGES-1-KO mice as compared with replicate WT mice (Figure 6). The metastatic phenotype observed in mPGES-1-KO mice was similar to that observed in MMP-2-KO mice, in which focal xenograft propagation and lung metastasis of LLC cells were reduced [44]. In agreement, MMP-2, as well as MMP-9, expression in the metastasized lung tissues was markedly lower in mPGES-1-KO mice than in WT mice (Figures 6D and 6E). Thus, in the metastatic foci, the PGE_2 derived from the host mPGES-1 may lead to the increase in the activities of MMP-2 and -9, which, in co-operation with VEGF, may promote the invasion of cancerous cells into the adjacent and distant tissues, thereby allowing subsequent expansion and metastasis of the tumour.

In conclusion, the results of the present study suggest that both cancer cell-associated and host-derived mPGES-1 is critical for tumour growth and metastasis. The mPGES-1-driven PGE_2 signalling on stromal cells may be functionally linked to the induction of potent pro-angiogenic and matrix-degrading factors, which in turn would facilitate tumour development. Previous studies have shown that, unlike the specific inhibition of COX-2, which predisposes to cardiovascular risk, gene ablation of mPGES-1 in mice shows minimal unfavourable effects on the circulation system [12]. Therefore an mPGES-1 inhibitor would exhibit a chemopreventive action on various tumours by attenuating both cancer cell- and stromal cell-derived PGE_2, thereby serving as a novel therapeutic tool for cancer. Future clinical studies will address the important question of the efficacy and safety of mPGES-1 inhibition in human diseases.

AUTHOR CONTRIBUTION

Daisuke Kamei designed and performed the experiments, analysed the data and contributed to writing the manuscript; Yuka Sasaki also performed the experiments; Yoshihito Nakatani, Masataka Majima, Yukio Ishikawa and Toshiharu Ishii helped in manuscript and scientific discussions; Satoshi Uematsu and Shizuo Akira provided the resources for the work; Ichiro Kudo designed the experiments; and Makoto Murakami and Shuntaro Hara designed the experiments and also wrote the manuscript.

ACKNOWLEDGEMENTS

We would like to thank Dr S. Oh-Ish (Kitasato Institute, Saitama, Japan) for providing us with helpful suggestions.

FUNDING

This work was supported in part by a Showa University Special Grant-in-Aid for Innovative Collaborative Research Projects; Grants-in-Aid for Scientific Research and "High-Tech Research Center" Project for Private Universities [matching fund subsidy (2004–2007)] from the Ministry of Education, Science, Culture, Sports and Technology of Japan; Grants-in-Aid for Comprehensive Research on Aging and Health from the Ministry of Health, Labour and Welfare of Japan; the Japan Society for the Promotion of Science for Young Scientists (a Research Fellowship to D.K.); and PRESTO from the Japan Science and Technology Agency (to M.M.)

REFERENCES

1 Levy, G. N. (1997) Prostaglandin H synthases, nonsteroidal anti-inflammatory drugs, and colon cancer. FASEB J. **11**, 234–247
2 Sheng, H., Shao, J., Washington, M. and DuBois, R. N. (2001) Prostaglandin E_2 increases growth and motility of colorectal carcinoma cells. J. Biol. Chem. **276**, 18075–18081
3 Murakami, M. and Kudo, I. (2004) Recent advances in molecular biology and physiology of the prostaglandin E_2-biosynthetic pathway. Prog. Lipid Res. **43**, 3–35
4 Tsujii, M. and DuBois, R. N. (1995) Alterations in cellular adhesion and apoptosis in epithelial cells overexpressing prostaglandin endoperoxide synthase 2. Cell **83**, 493–501
5 Tsujii, M., Kawano, S., Tsuji, S., Sawaoka, H., Hori, M. and DuBois, R. N. (1998) Cyclooxygenase regulates angiogenesis induced by colon cancer cells. Cell **93**, 705–716
6 Jakobsson, P. J., Thoren, S., Morgenstern, R. and Samuelsson, B. (1999) Identification of human prostaglandin E synthase: a microsomal, glutathione-dependent, inducible enzyme, constituting a potential novel drug target. Proc. Natl. Acad. Sci. U.S.A. **96**, 7220–7225
7 Murakami, M., Naraba, H., Tanioka, T., Semmyo, N., Nakatani, Y., Kojima, F., Ikeda, T., Fueki, M., Ueno, A., Oh-ishi, S. and Kudo, I. (2000) Regulation of prostaglandin E_2 biosynthesis by inducible membrane-associated prostaglandin E2 Synthase that acts in concert with cyclooxygenase-2. J. Biol. Chem. **275**, 32783–32792
8 Tanioka, T., Nakatani, Y., Semmyo, N., Murakami, M. and Kudo, I. (2000) Molecular identification of cytosolic prostaglandin E_2 synthase that is functionally coupled with cyclooxygenase-1 in immediate prostaglandin E_2 biosynthesis. J. Biol. Chem. **275**, 32775–32782
9 Tanikawa, N., Ohmiya, Y., Ohkubo, H., Hashimoto, K., Kangawa, K., Kojima, M., Ito, S. and Watanabe, K. (2002) Identification and characterization of a novel type of membrane-associated prostaglandin E synthase. Biochem. Biophys. Res. Commun. **291**, 884–889
10 Mancini, J. A., Blood, K., Guay, J., Gordon, R., Claveau, D., Chan, C. C. and Riendeau, D. (2001) Cloning, expression, and up-regulation of inducible rat prostaglandin E synthase during lipopolysaccharide-induced pyresis and adjuvant-induced arthritis. J. Biol. Chem. **276**, 4469–4475
11 Stichtenoth, D. O., Thoren, S., Bian, H., Peters-Golden, M., Jakobsson, P. J. and Crofford, L. J. (2001) Microsomal prostaglandin E synthase is regulated by proinflammatory cytokines and glucocorticoids in primary rheumatoid synovial cells. J. Immunol. **167**, 469–474
12 Samuelsson, B., Morgenstern, R. and Jakobsson, P. J. (2007) Membrane prostaglandin E synthase-1: a novel therapeutic target. Pharmacol. Rev. **59**, 207–224
13 Kamei, D., Yamakawa, K., Takegoshi, Y., Mikami-Nakanishi, M., Nakatani, Y., Oh-Ishi, S., Yasui, H., Azuma, Y., Hirasawa, N., Ohuchi, K. et al. (2004) Reduced pain hypersensitivity and inflammation in mice lacking microsomal prostaglandin E synthase-1. J. Biol. Chem. **279**, 33684–33695
14 Kamei, D., Murakami, M., Nakatani, Y., Ishikawa, Y., Ishii, T. and Kudo, I. (2003) Potential role of microsomal prostaglandin E synthase-1 in tumorigenesis. J. Biol. Chem. **278**, 19396–19405
15 Golijanin, D., Tan, J. Y., Kazior, A., Cohen, E. G., Russo, P., Dalbagni, G., Auborn, K. J., Subbaramaiah, K. and Dannenberg, A. J. (2004) Cyclooxygenase-2 and microsomal prostaglandin E synthase-1 are overexpressed in squamous cell carcinoma of the penis. Clin. Cancer Res. **10**, 1024–1031

16 Oshima, H., Oshima, M., Inaba, K. and Taketo, M. M. (2004) Hyperplastic gastric tumors induced by activated macrophages in COX-2/mPGES-1 transgenic mice. EMBO J. **23**, 1669–1678
17 Oshima, M., Oshima, H., Matsunaga, A. and Taketo, M. M. (2005) Hyperplastic gastric tumors with spasmolytic polypeptide-expressing metaplasia caused by tumor necrosis factor-α-dependent inflammation in cyclooxygenase-2/microsomal prostaglandin E synthase-1 transgenic mice. Cancer Res. **65**, 9147–9151
18 Hanahan, D. and Folkman, J. (1996) Patterns and emerging mechanisms of the angiogenic switch during tumorigenesis. Cell **86**, 353–364
19 Majima, M., Hayashi, I., Muramatsu, M., Katada, J., Yamashina, S. and Katori, M. (2000) Cyclo-oxygenase-2 enhances basic fibroblast growth factor-induced angiogenesis through induction of vascular endothelial growth factor in rat sponge implants. Br. J. Pharmacol. **130**, 641–649
20 Williams, C. S., Tsujii, M., Reese, J., Dey, S. K. and DuBois, R. N. (2000) Host cyclooxygenase-2 modulates carcinoma growth. J. Clin. Invest. **105**, 1589–1594
21 Murakami, M., Nakashima, K., Kamei, D., Masuda, S., Ishikawa, Y., Ishii, T., Ohmiya, Y., Watanabe, K. and Kudo, I. (2003) Cellular prostaglandin E_2 production by membrane-bound prostaglandin E synthase-2 via both cyclooxygenases-1 and -2. J. Biol. Chem. **278**, 37937–37947
22 Bombardier, C., Laine, L., Reicin, A., Shapiro, D., Burgos-Vargas, R., Davis, B., Day, R., Ferraz, M. B., Hawkey, C. J., Hochberg, M. C. et al. (2000) Comparison of upper gastrointestinal toxicity of rofecoxib and naproxen in patients with rheumatoid arthritis. N. Engl. J. Med. **343**, 1520–1528
23 Bresalier, R. S., Sandler, R. S., Quan, H., Bolognese, J. A., Oxenius, B., Horgan, K., Lines, C., Riddell, R., Morton, D., Lanas, A. et al. (2005) Cardiovascular events associated with rofecoxib in a colorectal adenoma chemoprevention trial. N. Engl. J. Med. **352**, 1092–1102
24 Narumiya, S., Sugimoto, Y. and Ushikubi, F. (1999) Prostanoid receptors: structures, properties, and functions. Physiol. Rev. **79**, 1193–1226
25 Steeg, P. S. (2006) Tumor metastasis: mechanistic insights and clinical challenges. Nat. Med. Rev. **12**, 895–904
26 Friedl, P. and Wolf, K. (2003) Tumour-cell invasion and migration: diversity and escape mechanisms. Nat. Rev. Cancer **3**, 362–374
27 Young, M. R. and Newby, M. (1986) Enhancement of Lewis lung carcinoma cell migration by prostaglandin E_2 produced by macrophages. Cancer Res. **46**, 160–164
28 Dohadwala, M., Batra, R. K., Luo, J., Lin, Y., Krysan, K., Pold, M., Sharma, S. and Dubinett, S. M. (2002) Autocrine/paracrine prostaglandin E_2 production by non-small cell lung cancer cells regulates matrix metalloproteinase-2 and CD44 in cyclo-oxygenase-2-dependent invasion. J. Biol. Chem. **277**, 50828–50833
29 Ito, H., Duxbury, M., Benoit, E., Clancy, T. E., Zinner, M. J., Ashley, S. W. and Whang, E. E. (2004) Prostaglandin E_2 enhances pancreatic cancer invasiveness through an Ets-1-dependent induction of matrix metalloproteinase-2. Cancer Res. **64**, 7439–7446
30 Pavlovic, S., Du, B., Sakamoto, K., Khan, K. M., Natarajan, C., Breyer, R. M., Dannenberg, A. J. and Falcone, D. J. (2006) Targeting prostaglandin E_2 receptors as an alternative strategy to block cyclooxygenase-2-dependent extracellular matrix-induced matrix metalloproteinase-9 expression by macrophages. J. Biol. Chem. **281**, 3321–3328
31 Sonoshita, M., Takaku, K., Sasaki, N., Sugimoto, Y., Ushikubi, F., Narumiya, S., Oshima, M. and Taketo, M. M. (2001) Acceleration of intestinal polyposis through prostaglandin receptor EP2 in *Apc* (*Delta 716*) knockout mice. Nat. Med. **7**, 1048–1051
32 Castellone, M. D., Teramoto, H., Williams, B. O., Druey, K. M. and Gutkind, J. S. (2005) Prostaglandin E_2 promotes colon cancer cell growth through a Gs-axin-β-catenin signaling axis. Science **310**, 1504–1510
33 Castellone, M. D., Teramoto, H. and Gutkind, J. S. (2006) Cyclooxygenase-2 and colorectal cancer chemoprevention: the β-catenin connection. Cancer Res. **66**, 11085–11088
34 Watanabe, K., Kawamori, T., Nakatsugi, S., Ohta, T., Ohuchida, S., Yamamoto, H., Maruyama, T., Kondo, K., Ushikubi, F., Narumiya, S. et al. (1999) Role of the prostaglandin E receptor subtype EP1 in colon carcinogenesis. Cancer Res. **59**, 5093–5096
35 Sung, Y. M., He, G. and Fischer, S. M. (2005) Lack of expression of the EP2 but not EP3 receptor for prostaglandin E_2 results in suppression of skin tumor development. Cancer Res. **65**, 9304–9311
36 Kawamori, T., Kitamura, T., Watanabe, K., Uchiya, N., Maruyama, T., Narumiya, S., Sugimura, T. and Wakabayashi, K. (2005) Prostaglandin E receptor subtype EP1 deficiency inhibits colon cancer development. Carcinogenesis **26**, 353–357
37 Pai, R., Soreghan, B., Szabo, I. L., Pavelka, M., Baatar, D. and Tarnawski, A. S. (2002) Prostaglandin E_2 transactivates EGF receptor: a novel mechanism for promoting colon cancer growth and gastrointestinal hypertrophy. Nat. Med. **8**, 289–293
38 Han, C., Demetris, A. J., Stolz, D. B., Xu, L., Lim, K. and Wu, T. (2006) Modulation of Stat3 activation by the cytosolic phospholipase $A_2\alpha$ and cyclooxygenase-2-controlled prostaglandin E_2 signaling pathway. J. Biol. Chem. **281**, 24831–24846
39 Sales, K. J., Maudsley, S. and Jabbour, H. N. (2004) Elevated prostaglandin EP2 receptor in endometrial adenocarcinoma cells promotes vascular endothelial growth factor expression via cyclic 3′,5′-adenosine monophosphate-mediated transactivation of the epidermal growth factor receptor and extracellular signal-regulated kinase 1/2 signaling pathways. Mol. Endocrinol. **18**, 1533–1545
40 Ansari, K. M., Sung, Y. M., He, G. and Fischer, S. M. (2007) Prostaglandin receptor EP2 is responsible for cyclooxygenase-2 induction by prostaglandin E_2 in mouse skin. Carcinogenesis **28**, 2063–2068
41 Nakanishi, M., Montrose, D. C., Clark, P., Nambiar, P. R., Belinsky, G. S., Claffey, K. P., Xu, D. and Rosenberg, D. W. (2008) Genetic deletion of mPGES-1 suppresses intestinal tumorigenesis. Cancer Res. **68**, 3251–3259
42 Elander, N., Ungerbäck, J., Olsson, H., Uematsu, S., Akira, S. and Söderkvist, P. (2008) Genetic deletion of mPGES-1 accelerates intestinal tumorigenesis in $APC^{Min/+}$ mice. Biochem. Biophys. Res. Commun. **372**, 249–253
43 Amano, H., Hayashi, I., Endo, H., Kitasato, H., Yamashina, S., Maruyama, T., Kobayashi, M., Satoh, K., Narita, M., Sugimoto, Y. et al. (2003) Host prostaglandin E_2-EP3 signaling regulates tumor-associated angiogenesis and tumor growth. J. Exp. Med. **197**, 221–232
44 Itoh, T., Tanioka, M., Yoshida, H., Yoshioka, T., Nishimoto, H. and Itohara, S. (1998) Reduced angiogenesis and tumor progression in gelatinase A-deficient mice. Cancer Res. **58**, 1048–1051

Received 8 January 2009/8 October 2009; accepted 21 October 2009
Published as BJ Immediate Publication 21 October 2009, doi:10.1042/BJ20090045

Biochem. J. (2010) **425**, 361–371 (Printed in Great Britain) doi:10.1042/BJ20090045

online data

SUPPLEMENTARY ONLINE DATA

Microsomal prostaglandin E synthase-1 in both cancer cells and hosts contributes to tumour growth, invasion and metastasis

Daisuke KAMEI*†, Makoto MURAKAMI*‡§, Yuka SASAKI*, Yoshihito NAKATANI*, Masataka MAJIMA‖, Yukio ISHIKAWA¶, Toshiharu ISHII¶, Satoshi UEMATSU**, Shizuo AKIRA**, Shuntaro HARA*[1] and Ichiro KUDO*[2]

*The Department of Health Chemistry, School of Pharmacy, Showa University, 1-5-8 Hatanodai, Shinagawa-ku, Tokyo 142-8555, Japan, †Department of Research and Development for Innovative Medical Needs, School of Pharmacy, Showa University, 1-5-8 Hatanodai, Shinagawa-ku, Tokyo 142-8555, Japan, ‡Tokyo Metropolitan Institute of Medical Science, 2-1-6 Kanikitazawa, Setagaya-ku, Tokyo 156-8506, Japan, §PRESTO, Japan Science and Technology Agency, 4-1-8 Honcho Kawaguchi, Saitama 332-0012, Japan, ‖Department of Pharmacology, School of Medicine, Kitasato University, 1-15-1 Kitasato, Sagamihara, Kanagawa 228-8555, Japan, ¶Department of Pathology, School of Medicine, Toho University, 5-21-16 Omori-Nishi, Ohta-ku, Tokyo 143-8540, Japan, and **Department of Host Defense, Research Institute for Microbial Diseases, Osaka University, 3-1 Yamada-oka, Suita, Osaka 565-0871, Japan

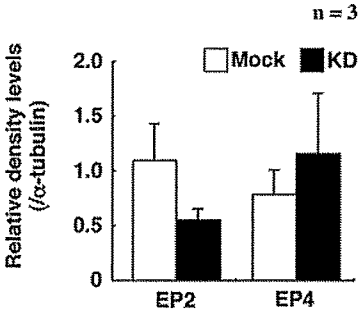

Figure S1 Reduced expression level of EP2 protein in mPGES-1-silenced LLC cells *in vitro*

Expression of EP2 and EP4 in mPGES-1-KD and control (mock) cells was assessed by immunoblotting. Representative results of at least three experiments are shown. On Western blot analysis the expression levels of EP2 and EP4 protein were quantified by a densitometer, with the expression level of α-tubulin used for normalization (means $\pm$ S.D., $n = 3$).

Received 8 January 2009/8 October 2009; accepted 21 October 2009
Published as BJ Immediate Publication 21 October 2009, doi:10.1042/BJ20090045

[1] To whom correspondence should be addressed (email haras@pharm.showa-u.ac.jp).

[2] Professor Kudo died on April 27, 2008. We greatly miss him as a scientist and a friend. We offer sincere thanks to all the friends, colleagues and former collaborators of Professor Kudo who showed him kindness during his lifetime.

Biochimie xxx (2010) 1–9

Contents lists available at ScienceDirect

Biochimie

journal homepage: www.elsevier.com/locate/biochi

Review

Prostaglandin E synthases: Understanding their pathophysiological roles through mouse genetic models☆

Shuntaro Hara [a,*], Daisuke Kamei [a,b], Yuka Sasaki [a], Akemi Tanemoto [a], Yoshihito Nakatani [a], Makoto Murakami [c]

[a] Department of Health Chemistry, School of Pharmaceutical Sciences, Showa University, 1-5-8 Hatanodai, Shinagawa-ku, Tokyo 142-8555, Japan
[b] Department of Research and Development for Innovative Medical Needs, School of Pharmaceutical Sciences, Showa University, Tokyo, Japan
[c] Biomembrane Signaling Project, The Tokyo Metropolitan Institute of Medical Science, Tokyo, Japan

ARTICLE INFO

Article history:
Received 30 November 2009
Accepted 9 February 2010
Available online xxx

Keywords:
Prostaglandin E synthase
mPGES-1
Knockout mice
PGE_2
Inflammation

ABSTRACT

Prostaglandin E synthase (PGES), which converts cyclooxygenase (COX)-derived prostaglandin H_2 (PGH_2) to PGE_2, is known to comprise a group of at least three structurally and biologically distinct enzymes. Two of them are membrane-bound and have been designated as mPGES-1 and mPGES-2. mPGES-1 is a perinuclear protein that is markedly induced by proinflammatory stimuli and downregulated by anti-inflammatory glucocorticoids as in the case of COX-2. It is functionally coupled with COX-2 in marked preference to COX-1. mPGES-2 is synthesized as a Golgi membrane-associated protein, and the proteolytic removal of the N-terminal hydrophobic domain leads to the formation of a mature cytosolic enzyme. This enzyme is rather constitutively expressed in various cells and tissues and is functionally coupled with both COX-1 and COX-2. Cytosolic PGES (cPGES) is constitutively expressed in a wide variety of cells and is functionally linked to COX-1 to promote immediate PGE_2 production. Recently, mice have been engineered with specific deletions in each of these three PGES enzymes. In this review, we summarize the current understanding of the *in vivo* roles of PGES enzymes by knockout mouse studies and provide an overview of their biochemical properties.

1. Introduction

Prostaglandin E_2 (PGE_2) is the most common prostanoid produced by a variety of cells and tissues and has a broad range of biological activity. Three kinds of enzymes – phospholipase A_2 (PLA_2), cyclooxygenase (COX), and terminal PGE synthase (PGES) – are involved in the biosynthesis of PGE_2, and each of the three enzymatic steps involves multiple enzymes that can act in different phases of cell activation [1–5]. Arachidonic acid (AA) released from membrane glycerophospholipids by PLA_2 enzymes is then supplied to either of the two COX isozymes, COX-1 or COX-2. The constitutive COX-1 contributes mainly to immediate PG generation, whereas the inducible COX-2 mediates delayed PG generation (Fig. 1). The COX metabolite PGH_2 is then isomerized to PGE_2 by terminal PGES enzymes.

To date, three PGES enzymes, microsomal PGES-1 (mPGES-1) and -2 (mPGES-2) and cytosolic PGES (cPGES), have been identified [6–9]. Recently, mice with specific deletions in each of these three PGES enzymes have been engineered; these knockout mice have provided models to elucidate the physiological and pathophysiological roles of these enzymes [10–15]. This review summarizes the current understanding of the *in vivo* roles of PGES enzymes as revealed by experiments using knockout mice including a discussion of their biological structures and transcriptional regulation (Table 1).

2. mPGES-1

2.1. Biochemical properties of mPGES-1

In 1999, mPGES-1 was the first PGES identified. Jakobsson et al. reported that the recombinant human microsomal glutathione (GSH) *S*-transferase (GST) 1-like 1, a member of the MAPEG (membrane-associated proteins involved in eicosanoid and glutathione metabolism) superfamily that had been listed in nucleic acid data bases, can catalyze the conversion of PGH_2 to PGE_2 with strict substrate specificity [6]. We also cloned rat and mouse orthologs of this protein and showed that this enzyme is identical to

☆ The research reviewed in this paper was supported in part by Grants-in-Aid for Scientific Research and the "High-Tech Research Center" Project for Private Universities (matching fund subsidy (2004–2007)) from the Ministry of Education, Culture, Sports, Science, and Technology of Japan; and by Grants-in-Aid for Comprehensive Research on Aging and Health, and Research on Dementia from the Ministry of Health, Labor, and Welfare of Japan.

* Corresponding author. Tel.: +81 3 3784 8196; fax: +81 3 3784 8245.
E-mail address: haras@pharm.showa-u.ac.jp (S. Hara).

0300-9084/$ – see front matter © 2010 Elsevier Masson SAS. All rights reserved.
doi:10.1016/j.biochi.2010.02.007

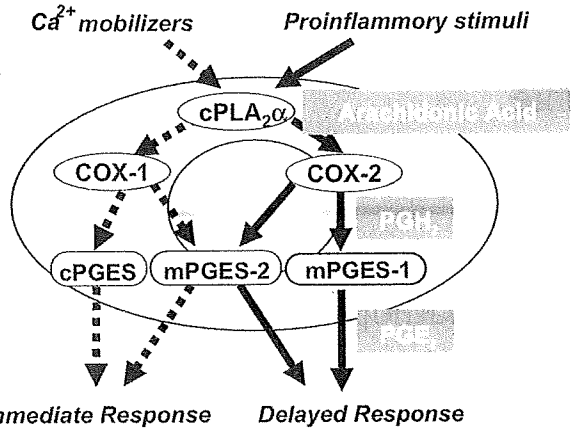

Fig. 1. Functional coupling of COX and PGES. Arachidonic acid released from membrane glycerophospholipids by cPLA$_2\alpha$ is then supplied to either of the two COX isozymes, COX-1 or COX-2. COX-1, a constitutive COX isozyme, contributes mainly to immediate PG generation in response to the Ca^{2+} mobilizer, whereas COX-2, an inducible enzyme, mediates delayed PG generation in response to proinflammatory stimuli. The COX metabolite PGH_2 is then isomerized to PGE_2 by three terminal PGES, mPGES-1, mPGES-2 and cPGES. mPGES-1 is functionally coupled with COX-2 in marked preference to COX-1, whereas cPGES is coupled preferentially with COX-1. mPGES-2 functions equally well with both COX-1 and COX-2.

a membrane-associated PGES, which we had originally detected in lipopolysaccharide (LPS)-stimulated macrophages [8].

mPGES-1 consists of 152–153 amino acids and shows significant homology with other MAPEG superfamily proteins, including MGST-1, MGST-2, MGST-3, 5-lipoxygenase-activating protein (FLAP), and leukotriene C_4 synthase (LTCS), with the highest homology being found with MGST-1 (38%). Furthermore, a projected structure of mPGES-1 at 10 Å revealed similar structural properties as had been determined for MGST-1, suggesting that the enzyme is a trimer of four helix bundles in which the hydrophobic helices traverse the membrane [16]. It was also shown that mutation of Arg^{110} in mPGES-1, which is the residue strictly conserved in all MAPEG protein, abrogates its catalytic function, implying this residue has an essential role [8].

mPGES-1 requires GSH as an essential cofactor for activity [6,8]. Purified recombinant mPGES-1 catalyzes rapid GSH-dependent conversion of PGH_2 to PGE_2 with a V_{max} of 170 μmol/min/mg and a high k_{cat}/K_m of 310 min^{-1} s^{-1} [16]. The enzyme also catalyzes GSH-dependent conversion of PGG_2 to 15-hydroperoxy-PGE_2. It displays weak GSH-dependent peroxidase activity toward cumene hydroperoxide, 5-hydroperoxyeicosatetraenoic acid, and 15-hydroperoxy-PGE_2 and catalyzes slow but significant conjugation of 1-chloro-2,4-dinitrobenzene to GSH.

2.2. Expression, transcriptional regulation, and cellular function of mPGES-1

Among PGES enzymes, only mPGES-1 is markedly induced by proinflammatory stimuli. Although the steady-state expression of mPGES-1 in normal rat tissues is very low, administration of LPS leads to a dramatic increase in mPGES-1 expression in various tissues [8,17,18]. Stimulation of various cultured cells with proinflammatory stimuli leads to a marked elevation of mPGES-1 expression, often with concomitant induction of COX-2. Concordant upregulation of COX-2 and mPGES-1 is accompanied by a marked increase in PGE_2 production [8,17,19–21]. It has also been shown that the coordinate upregulation of COX-2 and mPGES-1 and the attendant PGE_2 generation are downregulated by anti-inflammatory glucocorticoid [8,17,19,21]. However, there are some differences in the kinetics of induction between COX-2 and mPGES-1 [21], suggesting that the regulatory mechanisms for their expression are distinct. The promoter of the human mPGES-1 gene is GC-rich but lacks a TATA box, unlike the COX-2 gene promoter [22]. Furthermore, the 3′ region of the mPGES-1 gene lacks the AUUUA mRNA instability sequences that are found in the COX-2 gene. Our gene promoter analysis revealed that stimulus-inducible mPGES-1 expression required tandem GC boxes adjacent to the initiation site and that the inducible transcription factor Egr-1 is activated and bound to this GC box, leading to inducible mPGES-1 transcription.

It is also noteworthy that mPGES-1 is functionally coupled with COX-2, in marked preference to COX-1. When COX-2 and mPGES-1 are co-transfected into HEK293 cells, considerable amounts of PGE_2 are produced from both endogenous and exogenous AA relative to cells transfected with either enzyme alone [8]. In comparison, coupling between COX-1 and mPGES-1 occurs only when a large amount of AA is supplied exogenously, or if burst activation of cytosolic PLA$_2\alpha$ takes place, endogenously. Our co-transfection experiments revealed that mPGES-1 colocalized with both COX-1 and COX-2 in the perinuclear membrane [8]. The mechanism whereby mPGES-1 favors COX-2 over COX-1 cannot be explained simply by their subcellular localizations, but the presence of microdomains, in which mPGES-1 is located in closer proximity to COX-2 than to COX-1, within the perinuclear compartment cannot be ruled out. Colocalization of COX-2 and mPGES-1 in such a microdomain may allow efficient transfer of the unstable substrate PGH_2 between them. Further support for the COX-2/mPGES-1 coupling has been provided by studies using an antisense oligonucleotide or a small interfering RNA, in which the mPGES-1 knockdown markedly attenuates COX-2-mediated PGE_2 production in cultured cells [23,24].

2.3. Possible in vivo functions of mPGES-1

The first report of the critical role of mPGES-1 for induced PGE_2 production *in vivo* was published in 2002 [10]. Those authors generated mPGES-1-deficient mice and demonstrated that the biosynthesis of PGE_2 in wild-type peritoneal macrophages induced by LPS was abolished in mPGES-1-deficient cells. It was also shown that the increase in serum PGE_2 concentration by intraperitoneal administration of LPS was also suppressed in mPGES-1-deficient mice, although mPGES-1-deficient mice showed normal responses to the LPS-induced shock. Following this report, several investigators

Table 1
Characteristics of three PGES enzymes.

	mPGES-1	cPGES	mPGES-2
Gene map locus (human)	9q34.4	12q13.13	9q33–q34
Transcriptional regulation	Inducible	Constitutive	Constitutive
Protein molecular weight	16 kDa	23 kDa	33 kDa
Amino acid composition	152–153 aa	160 aa	377–384 aa
Subcellular localization	Perinuclear membrane	Cytoplasm	Golgi, cytoplasm
Preference for COX isozymes	COX-2 > COX-1	COX-1 > COX-2	No preference
Phenotypic changes in KO mice	Reduced inflammatory reactions, Impaired pain and febrile response, Suppression of tumorigenesis, etc.	Perinatal-lethal with poor lung development, delayed skin maturation, and growth retardation	No specific phenotype

Please cite this article in press as: S. Hara, et al., Prostaglandin E synthases: Understanding their pathophysiological roles through mouse genetic models, Biochimie (2010), doi:10.1016/j.biochi.2010.02.007

established additional mPGES-1-deficient mouse lines in order to unveil possible *in vivo* functions of mPGES-1.

2.3.1. Role of mPGES-1 in inflammatory reactions

The induction both *in vitro* and *in vivo* of mPGES-1 following proinflammatory stimuli, such as interleukin-1 (IL-1), tumor necrosis factor (TNF), and LPS, strongly suggests that mPGES-1 is an essential component of PGE_2 production during inflammatory reactions [6,8,17–21]. It has also been shown that mPGES-1 is abundantly expressed in synovial cells of patients with rheumatoid arthritis [23] and in the hind paws of rats with adjuvant arthritis [17]. We and others have shown that mPGES-1 plays an important role in synovial inflammation using mPGES-1-deficient mice. Trebino et al. induced arthritis by subcutaneous administration of chicken collagen type II and assessed symptoms of arthritis by clinical evaluation and histopathology [11]. They showed that in this collagen-induced arthritis (CIA) model, mPGES-1-deficient mice developed no or little arthritis. Similar CIA phenotypes have been observed in mice lacking $cPLA_2\alpha$ [24], COX-2 [25] or the PGE receptor EP4 [26], thus revealing the metabolic flow of the $cPLA_2\alpha$/COX-2/mPGES-1/EP4 pathway, leading to the development of inflammatory arthritis. It is possible that the results found in the CIA model are influenced in part by inadequate proximal lymphocyte-mediated responses in addition to the synovial symptoms, since the anti-collagen antibody formation in COX-2-deficient mice revealed a remarkable decrease in this humoral response. This view was further supported by the fact that COX-2-deficient mice exhibited altered helper T-cell development, a process that PGE_2 reversed [27]. Subsequently, it was indeed found that defective generation of a humoral immune response was associated with a reduced incidence and severity of the CIA model in mPGES-1-null mice [28]. Using the collagen antibody-induced arthritis (CAIA) model, in which the influence of lymphocyte-mediated humoral responses could be minimal, we also showed that the severity of synovial inflammation, including bone destruction and juxta-articular bone loss, were mild in mPGES-1-deficient mice as compared with replicate wild-type mice, although the incidence of inflammation was unaffected (Fig. 2A) [29]. mPGES-1-mediated PGE_2 production by osteoblasts plays a critical role in LPS-induced bone loss associated with inflammation [30,31]. Moreover, mPGES-1 deficiency was associated with impaired fracture healing, but not with bone loss or osteoarthritis, in mouse models of skeletal disorders [32].

Antigen-induced paw edema was markedly reduced in mPGES-1-deficient mice as compared with replicate wild-type mice [11]. This deficit in edema was accompanied by a marked reduction in the infiltration of white blood cells into the inflamed site. Likewise, the migration of macrophages following peritoneal injection of thioglycollate was strikingly reduced in mPGES-1-null mice relative to replicate wild-type mice [29]. We recently found that exudate accumulation and leukocyte migration into the pleural cavity after intrapleural injection of carrageenan was also attenuated in mPGES-1-deficient mice (Fig. 2B). These observations indicate that mPGES-1-derived PGE_2 increases vascular permeability in acute inflammatory reactions.

The formation of inflammatory granulation tissue and attendant angiogenesis in the dorsum induced by subcutaneous implantation of a cotton thread was significantly reduced in mPGES-1 knockout mice as compared with wild-type mice [29]. In this model, mPGES-1 deficiency was also associated with reduced induction of vascular endothelial cell growth factor (VEGF) in the granulation tissue. These results indicated that mPGES-1-derived PGE_2, in cooperation with VEGF, may play a critical role in the development of inflammatory granulation and angiogenesis, thus eventually contributing to tissue remodeling.

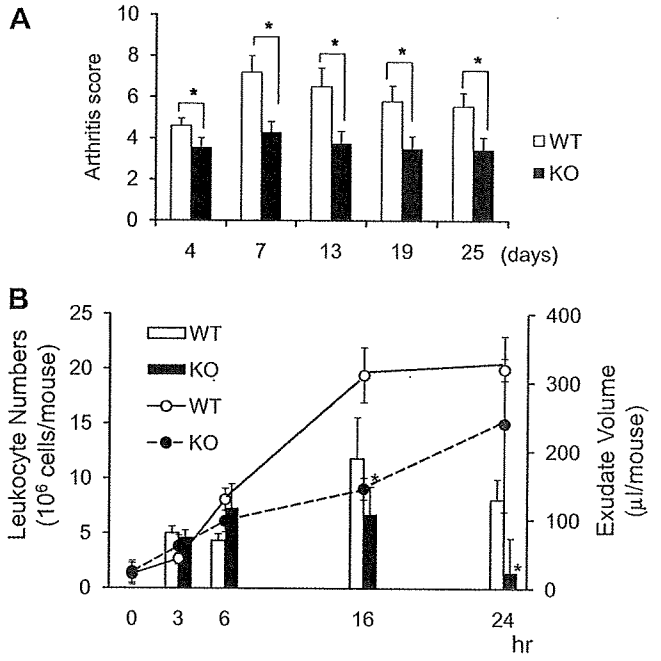

Fig. 2. Impaired inflammatory reactions in mPGES-1 knockout mice. A. mPGES-1 knockout and wild-type mice were injected intraperitoneally with 10 mg of anti-collagen monoclonal antibodies on day 0 and boosted with 50 μg of LPS on days 2 and 7, followed by intermittent LPS injections every 3 days. The clinical arthritis score was graded on a 0–3 scale as follows: 0, normal; 1, swelling of ankle or wrist, or limited to digits; 2, swelling of the entire paw; 3, maximal swelling. Each limb was graded, allowing a maximum arthritis score of 12 for each animal. Data were analyzed by Student's *t*-test. The results are expressed as means ± standard error ($n = 3$; *, $p < 0.05$ versus wild-type mice). For details, see Ref. [29]. B. mPGES-1 knockout and wild-type mice had been injected intrapleurally with 0.1 ml of 1% carrageenan saline solution. Immediately after the animals were killed by exsanguination at specified time points after the carrageenan injection, pleural exudates and saline wash (0.5 ml) were collected, and the exudate volume (bars) and leukocyte number in the exudates (lines) were measured. Data were analyzed by Student's *t*-test. The results are expressed as means ± standard error ($n = 3$–9; *, $p < 0.05$ versus wild-type mice).

2.3.2. Role of mPGES-1 in pain

PGE_2 is known to mediate inflammatory pain. The inflammatory pain response has been assessed using an acetic acid writhing model, in which diluted acetic acid was injected into the peritoneal cavity of mice. The pain response as recorded by counting the number of writhing motions was significantly reduced in mPGES-1-deficient mice compared with wild-type mice [11,29]. This phenotype was particularly evident when these mice were primed with LPS, where the stretching behavior and the peritoneal PGE_2 level were significantly reduced in knockout mice relative to wild-type mice [29]; this is being consistent with elevated expression of COX-2 and mPGES-1 in response to LPS. The basal (i.e., LPS-non-primed) writhing response was also partially reduced in mPGES-1-null mice [11,29], where COX-1-mPGES-1 coupling takes place.

The effect of mPGES-1 deficiency on neuropathic pain was also investigated in a neuropathic pain model prepared by spinal nerve transection [33]. The left L5 spinal nerve was transected, and after recovery, the mice were subjected thermal and mechanical sensitivity testing. The results showed that, unlike wild-type mice, mPGES-1-null mice did not exhibit mechanical allodynia or thermal hyperalgesia.

2.3.3. Role of mPGES-1 in fever

Genetic inactivation of COX-2, but not of COX-1, reduced PGE_2 levels in the central nervous system (CNS), in association with impaired LPS-induced febrile response [34]. Likewise, mPGES-1

Please cite this article in press as: S. Hara, et al., Prostaglandin E synthases: Understanding their pathophysiological roles through mouse genetic models, Biochimie (2010), doi:10.1016/j.biochi.2010.02.007

knockout mice showed no fever and no central PGE_2 synthesis after peripheral injection of LPS [35]. It was also shown that injection of PGE_2 into the brain ventricles elicited a fever response in mPGES-1 knockout mice. In rats, LPS treatment led to an increase in mPGES-1 expression in blood vessels, especially in veins and venules, in the whole brain [18]. Thus, cerebral vascular endothelial cells express components enabling blood-borne cytokines to stimulate the synthesis of PGE_2, whose small size and lipophilic property allow it to pass across the blood–brain barrier and to diffuse into the CNS neurons, thereby evoking the febrile response. Furthermore, Saha et al. reported that both induction of febrile responses by subcutaneous injection of turpentine (a model for an aseptic cytokine-induced pyresis) and intraperitoneal injection of IL-1β were also strongly impaired in mPGES-1-deficient mice [36]. In contrast, wild-type and mPGES-1-deficient mice showed similar psychogenic stress-induced hyperthermia, diurnal temperature variations, and reduced motor activity following injection of turpentine. These results indicate that mPGES-1-derived PGE_2 plays a critical role in fever during infectious and inflammatory conditions but is functionally dissociated from circadian temperature regulation, stress-induced hyperthermia, and inflammation-induced activity depression.

2.3.4. Role of mPGES-1 in neurological disorders

The role of PGE_2 in brain diseases, including ischemic injury and several neurodegenerative diseases has been established in models using mice lacking individual PGE receptors [37]. Ikeda-Matsuo et al. demonstrated that mPGES-1 was induced in neurons, microglia, and endothelial cells in the cerebral cortex after transient focal ischemia and indicated that mPGES-1-derived PGE_2 may be a critical determinant of postischemic neurological dysfunctions [38]. In mPGES-1 knockout mice, in which postischemic PGE_2 production in the cortex was completely absent, infarction, edema, apoptotic cell death, and caspase-3 activation in the cortex after ischemia were all reduced compared with those in wild-type mice. Furthermore, the behavioral neurological dysfunctions observed after ischemia in wild-type mice were significantly ameliorated in mPGES-1 knockout mice.

Induction of mPGES-1 was observed in various areas and various kinds of cells in the brain. Treatment of rat astrocytes with β-amyloid also induced mPGES-1 expression [39]. In clinical views, treatment with COX inhibitors slowed progression of Alzheimer's disease, and both COX-2 expression and PGE_2 levels were elevated in brains from Alzheimer's disease patients [40,41]. A recent immunohistochemical analysis revealed that mPGES-1 expression was also elevated in the brains of patients with Alzheimer's disease [42]. In this context, mPGES-1 might participate in the progression of Alzheimer's disease.

2.3.5. Role of mPGES-1 in tumorigenesis

COX-2 plays a critical role in the development of colorectal cancer and likely other types of cancer [43]. Pharmacological or genetic inactivation of COX-2 led to the suppression of cell growth and survival as well as to reductions in tumor size, invasion, and metastasis [44]. Disruption of $cPLA_2\alpha$ [45] or the PGE receptor EP2 [46] also resulted in a reduced incidence of gastrointestinal polyps, providing strong evidence for a link between PGE_2 signaling and oncogenesis. The tumorigenic potential of mPGES-1 has been suggested by several observations: that transfection of mPGES-1 in combination with COX-2, but not with COX-1, into HEK293 cells led to cellular transformation with a concomitant increase in PGE_2 [8]; that the COX-2/mPGES-1-co-transfected cells formed a number of large colonies in soft agar culture and were tumorigenic when implanted into nude mice [47]; and that transgenic mice overexpressing both COX-2 and mPGES-1 developed metaplasia, hyperplasia, and tumorous growth in the glandular stomach with heavy macrophage infiltration [48]. We recently showed that PGE_2 synthesis, cell proliferation and invasive activity *in vitro* and xenograft formation *in vivo* were reduced by mPGES-1 knockdown and conversely enhanced by mPGES-1 overexpression in Lewis lung carcinoma (LLC) cells [49].

Furthermore, we recently found that, like cancer cell-associated mPGES-1, host-associated mPGES-1 contributes to tumor growth, invasion, and metastasis using mPGES-1-deficient mice [49]. LLC tumors grafted subcutaneously into mPGES-1 knockout mice grew more slowly than did those grafted into wild-type mice, with concomitant decreases in the density of microvascular networks, the expression of proangiogenic VEGF, and the activity of matrix metalloproteinase-2. Lung metastasis of intravenously injected LLC cells was also significantly less obvious in mPGES-1 knockout mice than in wild-type mice. mPGES-1-driven PGE_2 signaling on host stromal cells may be functionally linked to the induction of potent proangiogenic and matrix-degrading factors, which in turn would facilitate tumor development.

The effect of mPGES-1 deficiency on intestinal tumorigenesis was also reported. Nakanishi et al. showed that the genetic deletion of mPGES-1 ameliorated the development of intestinal tumors in both $Apc^{\Delta 14}$-dependent and carcinogen-induced models [50]. In contrast, Elander et al. demonstrated that intestinal polyposis was exacerbated in mPGES-1-null Apc^{Min} mutant mice, probably because of the metabolic shift from PGE_2 toward other pro-tumorigenic lipid mediators [51]. Although the reason for the discrepancy between these two studies is unclear, our recent results appear to be in line with those of the former study.

2.3.6. Role of mPGES-1 in cardiovascular diseases

The selective inhibition, knockout, or mutation of COX-2, or the deletion of the receptor for COX-2-derived PGI_2, accelerates thrombogenesis and elevates blood pressure in mice, whereas these responses are attenuated by COX-1 knockdown, which mimics the beneficial effects of low-dose aspirin. The deletion of mPGES-1 in mice reduced PGE_2 and increased PGI_2 in circulation, had no effect on thromboxane biosynthesis, and affected neither thrombogenesis nor blood pressure [52]. Furthermore, the deletion of mPGES-1 led to eccentric cardiac myocyte hypertrophy, left ventricular dilation, and impaired left ventricular contractile function after acute myocardial infarction [53]. In mice with a low-density lipoprotein receptor knockout background, the deletion of mPGES-1 also augmented PGI_2 and retarded atherosclerosis development without an attendant impact on blood pressure [54], and protected against abdominal aortic aneurysm formation induced by angiotensin II in hyperlipidemic mice, coincident with a reduction in oxidative stress [55]. These results suggest that inhibitors of mPGES-1 may retain their anti-inflammatory efficacy by depressing PGE_2, while avoiding the adverse cardiovascular consequences associated with COX-2-mediated PGI_2 suppression.

2.3.7. Role of mPGES-1 in renal homeostasis

PGE_2 influences a wide range of physiologic functions in the kidney, and mPGES-1 colocalizes with both COX-1 and COX-2 in distal convoluted tubules, medullary interstitial cells, and cortical and medullary collecting ducts [56]. Although there was a 50% decrease in basal urinary excretion of PGE_2 in mPGES-1-null mice [57], these mice were similar to wild-type mice in their urinary osmolalities at baseline and after water deprivation, as well as in their blood pressure on control, high-salt, or low-salt diets [58]. In contrast, another study showed that mPGES-1-deficient mice developed severe and progressive hypertension associated with an inappropriate increase in sodium balance when fed a high-salt diet, with a marked reduction of urinary PGE_2 [59]. These mice exhibited a significantly impaired ability to excrete an acute enteral load of NaCl as well as a remarkable inhibition of high salt-induced increase in the gene expression of all three NO synthase isoforms. Chronic salt

Please cite this article in press as: S. Hara, et al., Prostaglandin E synthases: Understanding their pathophysiological roles through mouse genetic models, Biochimie (2010), doi:10.1016/j.biochi.2010.02.007

loading remarkably induced mPGES-1 protein expression exclusively in the distal nephron. In addition, mPGES-1 deficiency sensitized the hypertensive effect of angiotensin II. Overall, this study characterized the natriuretic and antihypertensive role of the mPGES-1/PGE_2/NO axis that likely contributes to blood pressure homeostasis.

It was also shown that mPGES-1 deletion impairs diuretic response to acute water loading [60]. Compared with wild-type mice, mPGES-1-null mice exhibited an impaired ability to excrete an acute water load, but not a chronic water load. In response to acute water loading, the renal aquaporin-2 protein level in wild-type mice was significantly reduced, but this reduction was blunted in mPGES-1-null mice. That study of mPGES-1-null mice also revealed a delayed increase in urinary PGE_2 excretion by acute water loading, coinciding with the stimulation of renal medullary expression of cPGES but not of mPGES-2. These results suggested that cPGES may act in concert with mPGES-1 to sustain renal PGE_2 production, particularly in the face of water excess.

2.3.8. Role of mPGES-1 in gastrointestinal homeostasis

PGE_2 is crucial for maintaining gastrointestinal mucosal homeostasis. Inflammatory bowel disease, including Crohn's disease and ulcerative colitis, is characterized by chronic, relapsing inflammation of the gastrointestinal tract. Increased amounts of PGE_2 were detected at sites of intestinal inflammation and correlated with disease activity [61], but COX inhibitors triggered or worsened the disease [62]. Experimental models for inflammatory bowel disease indicate that PGE_2 appears to have a dual effect. High levels of PGE_2 exacerbate the inflammatory process [63]. On the other hand, PGE_2 signaling is required for suppressing colitis symptoms and protecting mucosal damage. Mice engineered to be deficient in COX-2 or the PGE_2 receptor EP4 were sensitized to the development of experimental colitis, whereas treatment of EP4-selective agonist ameliorated colitis in wild-type mice [64,65]. mPGES-1 expression was also increased in inflamed intestinal mucosa from patients with inflammatory bowel disease [66]. To reveal whether or not mPGES-1 exhibits a beneficial role in mucosal protection, we examined the roles and functions of mPGES-1 in ulcerative colitis using a dextran sodium sulfate (DSS)-induced colitis model in mice (Fig. 3). Colitis was induced in wild-type or mPGES-1-deficient mice by continuous oral administration of 5% DSS in drinking water. DSS-induced expression of mPGES-1 was found throughout the large intestine in wild-type mice. The hemoccult scores of DSS-treated mPGES-1-deficient mice were significantly higher than those of wild-type mice, and mPGES-1-deficient mice exhibited significantly more severe anemia and splenomegaly than wild-type mice. The decrease in PGE_2 levels in descending colon and increased expression levels of proinflammatory cytokines were also found in mPGES-1-deficient mice. Furthermore, mPGES-1 deficiency induced severe epithelial loss and crypt abscess in the colon. These results indicate that mPGES-1-derived PGE_2 contributes to mucosal defense in colitis and negatively modulates acute colonic injury.

It was also shown that basal COX-1-dependent PGE_2 production in the stomachs of mPGES-1-deficient mice was decreased by 80–90% relative to that in wild-type mice [57], suggesting that COX-1/mPGES-1-derived PGE_2 might also contribute to the homeostatic protection of gastric mucosa.

2.3.9. Role of mPGES-1 in reproduction: a remaining mystery

Ovulation and fertilization are key steps in female reproduction, which, in turn, is regulated by several hormones, including gonadotropins. PGE_2, a dominant prostanoid in the ovary, has been implicated as a mediator of the ovulatory actions of gonadotropins. Gonadotropins induced COX-2 expression in granulosa cells of ovarian follicles prior to ovulation *in vivo* [67,68]. COX-2-deficient mice have a reduced ability to ovulate and severe problems in fertilization as well as defects in the uterus's ability to receive implants and to undergo decidualization [69]. Furthermore, studies using PGE receptor EP2-deficient mice revealed that PGE_2 cooperates with gonadotropins to complete cumulus expansion for successful fertilization [70,71]. Like COX-2, mPGES-1 was markedly upregulated in the granulose cell layer of bovine follicles after treatment with gonadotropins in the hours just prior to ovulation, a period when EP2 may be critically involved [72]. It was also reported that mPGES-1 is highly expressed in the female reproductive organs of various animal species, including humans [73–75]. However, mPGES-1-null mice showed no apparent reproduction abnormality [10,11], even under the inflammatory preterm delivery model in which mPGES-1 expression was markedly increased in the myometrium and fetal membrane [76].

Also, although both COX-2 and mPGES-1 were increased at the ductus arteriosus in perinatal mice [77] and patent ductus arteriosus and associated neonatal death occurred in EP4-deficient mice [78], this phenotype did not occur in mPGES-1-null mice probably due to compensation by mPGES-2 [79]. Thus, even though the contributions of mPGES-1 to these reproductive events are currently unclear, an mPGES-1 inhibitor may stand out as a better prospective tool than the currently used COX inhibitors for the management of pregnant women as well as premature infants with persistent ductus.

3. cPGES

3.1. Biochemical properties of cPGES

In 2000, we purified cPGES as a cytosolic form of PGES from LPS-treated rat brain and sequence analysis of the 23 kDa purified protein revealed that it is identical to the heat shock protein 90 (Hsp90)-associated protein p23 [7], which had been originally implicated as a cofactor for the molecular chaperone function of Hsp90 [80,81].

Like mPGES-1, cPGES requires GSH as an essential cofactor for its activity [7]. As with the classical cytosolic GSTs, cPGES activity is inhibited by 1-chloro-2,4-dinitrobenzene, even though 1-chloro-2,4-dinitrobenzene itself is a poor substrate for cPGES. Although the homology between cPGES and other known cytosolic GSTs is low, near its N-terminus cPGES has a tyrosine residue (Tyr^9) that is conserved in several other cytosolic GSTs. Tyr^9 mutation abrogates cPGES activity, suggesting that this tyrosine serves as a GSH acceptor, as it does in other cytosolic GSTs [82].

cPGES is directly associated with and phosphorylated by protein kinase CK2, resulting in a marked reduction of K_m for the substrate PGH_2 ($K_m = 66.6$ μM for cPGES alone compared to $K_m = 35.7$ μM for cPGES plus CK2) [83]. In activated cells, CK2-directed phosphorylation of cPGES occurs in parallel with increased cPGES enzymatic activity and PGE_2 production, and these processes are facilitated by interaction with Hsp90. cPGES, CK2, and Hsp90 form a stoichiometric complex of 1:1:1 immediately after cell activation. In this context, Hsp90 may act as an essential scaffold protein that brings cPGES and CK2 in proximity, thereby spatially allowing their efficient functional interaction under physiological conditions. *In vitro* coincubation of Hsp90, CK2 and cPGES results in maximal cPGES activity ($K_m = 14.9$ μM). On the other hand, pharmacologic inhibition of CK2 or Hsp90 or mutation of two CK2-directed phosphorylation sites (Ser^{113} and Ser^{118}) on cPGES results in poor activation of cPGES [83,84]. These results indicate that the tertiary complex formation and attendant phosphorylation are essential for cPGES to act in cells.

3.2. Expression and cellular function of cPGES

cPGES is expressed ubiquitously and in abundance in the cytosol of various tissues and cells [7]. Although the expression of cPGES is constitutive and is unaffected by proinflammatory stimuli in most

Please cite this article in press as: S. Hara, et al., Prostaglandin E synthases: Understanding their pathophysiological roles through mouse genetic models, Biochimie (2010), doi:10.1016/j.biochi.2010.02.007